AD-A120 047 ARMY ARMAMENT RESEARCH AND DEVELOPMENT COMMAND ABERD--ETC F/G 21/2
APPLICATION OF CARS TO OBTAIN TEMPERATURE IN FLAME ENVIRONMENTS--ETC(U)
AUG 82 J A VANDERHOFF, A J KOTLAR

UNCLASSIFIED ARBRL-TR-02417 SBI-AD-F300 080 NL

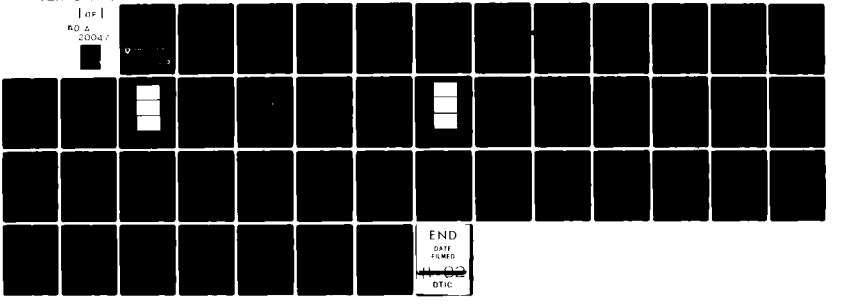

AF-F300080

(12)

AD

AD A120047

TECHNICAL REPORT ARBRL-TR-02417

APPLICATION OF CARS TO OBTAIN TEMPERATURE IN FLAME ENVIRONMENTS

John A. Vanderhoff
Anthony J. Kotlar

August 1982

US ARMY ARMAMENT RESEARCH AND DEVELOPMENT COMMAND
BALLISTIC RESEARCH LABORATORY
ABERDEEN PROVING GROUND, MARYLAND

UNCLASSIFIED

SECURITY CLASSIFICATION OF THIS PAGE (When Data Entered)

REPORT DOCUMENTATION PAGE		READ INSTRUCTIONS BEFORE COMPLETING FORM
1. REPORT NUMBER Technical Report ARBRL-TR-02417	2. GOVT ACCESSION NO. AD-A120047	3. RECIPIENT'S CATALOG NUMBER
4. TITLE (and Subtitle) Application of CARS to Obtain Temperature In Flame Environments		5. TYPE OF REPORT & PERIOD COVERED FINAL 6. PERFORMING ORG. REPORT NUMBER
7. AUTHOR(s) JOHN A. VANDERHOFF AND ANTHONY J. KOTLAR		8. CONTRACT OR GRANT NUMBER(s)
9. PERFORMING ORGANIZATION NAME AND ADDRESS USA Ballistic Research Laboratory ATTN: DRDAR-BLI Aberdeen Proving Ground, MD 21005		10. PROGRAM ELEMENT, PROJECT, TASK AREA & WORK UNIT NUMBERS 1L161101A91A
11. CONTROLLING OFFICE NAME AND ADDRESS US Army Armament Research & Development Command US Army Ballistic Research Laboratory (DRDAR-BL) Aberdeen Proving Ground, MD 21005		12. REPORT DATE August 1982 13. NUMBER OF PAGES 49
14. MONITORING AGENCY NAME & ADDRESS (if different from Controlling Office)		15. SECURITY CLASS. (of this report) UNCLASSIFIED 15a. DECLASSIFICATION/DOWNGRADING SCHEDULE

16. DISTRIBUTION STATEMENT (of this Report)

Approved for public release; distribution unlimited

17. DISTRIBUTION STATEMENT (of the abstract entered in Block 20, if different from Report)

18. SUPPLEMENTARY NOTES

19. KEY WORDS (Continue on reverse side if necessary and identify by block number)

Coherent Anti-Stokes Raman Spectroscopy
Flame Temperature
Premixed Flames
Laser Diagnostics

20. ABSTRACT (Continue on reverse side if necessary and identify by block number)

raj

A coherent anti-Stokes Raman scattering (CARS) experiment has been assembled and used to determine temperatures in various flame experiments. Using the Q-branch rotational-vibrational CARS signal from the N_2 molecule, temperature profiles in CH_4/air and CH_4/N_2O premixed flames have been obtained. Additionally temperatures have been determined for H_2 and CH_4 diffusion flames using the CARS signal from the Q-branch of H_2. Several possible experiments in ballistics (muzzle flash and propellant strand

DD FORM 1 JAN 73 1473 EDITION OF 1 NOV 65 IS OBSOLETE

UNCLASSIFIED

SECURITY CLASSIFICATION OF THIS PAGE (When Data Entered)

20. burning) are discussed in the report.

TABLE OF CONTENTS

LIST OF ILLUSTRATIONS

LIST OF TABLES

I. INTRODUCTION

The use of laser light to probe combustion processes has become a very active field of research. Because of the non-perturbing nature of light and the monochromicity of the laser, this tool is well suited for making detailed spatially and temporally resolved measurements in combustion environments. Raman techniques can be readily applied for probing combustion processes at elevated pressure since the Raman scattering processes occur on time scales less than 10^{-12}s, a time short compared to the collision times.

Spontaneous Raman spectroscopy has been used to probe relatively clean flame systems[1-9]; however, background noise effects such as luminosity, fluorescence, and particle incandescence can obscure the spontaneous Raman signals. With the development of very high power visible lasers, non-linear optical spectroscopy became feasible. Coherent anti-Stokes Raman scattering (CARS)[10-11] has emerged as one of the most promising techniques for probing

---

[1] *M. Lapp and C.M. Penney, Eds., Laser Raman Gas Diagnostics, Plenum Press, New York, 1973.*

[2] *S. Lederman, "The Use of Laser Raman Diagnostics in Flow Fields and Combustion," Prog. Energy Combust. Sci. Vol. 3, pp. 1-34 1977.*

[3] *M. Lapp, "Raman Scattering Measurements of Combustion Properties," Laser Probes for Combustion Chemistry, ACS Symposium Series 134, Washington, D.C., 1980.*

[4] *J.H. Bechtel, "Temperature Measurements of the Hydroxyl Radical and Molecular Nitrogen in Premixed Laminar Flames by Laser Techniques," Applied Optics Vol. 18, p. 2100, 1979.*

[5] *M. Bridoux, M. Crunell-Cras, F. Grase, and Michel Delhaye, "Use of Multichannel Pulsed Raman Spectroscopy as a Diagnostic Technique in Flames," Combustion and Flame, Vol. 36, pp. 109-116, 1979.*

[6] *M.C. Drake and G.M. Rosenblatt, "Rotational Raman Scattering from Premixed and Diffusion Flames," Combustion and Flame, Vol. 33, pp. 179-196, 1978.*

[7] *G. Alessandretti, "Some Results on the Measurement of Temperature and Density in a Flame by Raman Spectroscopy," Optica Acta, Vol. 27, pp. 1095-1103, 1980.*

[8] *A.A. Boiarski, R.H. Barnes, and J.F. Kircher, "Flame Measurements Utilizing Raman Scattering," Combustion and Flame, Vol. 32 pp. 111-114, 1978.*

[9] *D.P. Aeschliman, J.C. Cummings, and R.A. Hill, "Raman Spectroscopic Study of a Laminar Hydrogen Diffusion Flame in Air," J. Quant. Spectrosc. Radiat. Transfer Vol. 21, pp.293-307, 1979.*

[10] *A.C. Eckbreth, P.A. Boncsyk, and J.F. Verdieck, "Laser Raman and Fluorescence Techniques for Practical Combustion Diagnostics," Appl. Spectros. Reviews, Vol. 13, pp. 15-164, 1978.*

the more hostile combustion environments. Highly sooting flames[12], combustors[13,14], internal combustion engines[15], and gun propellant flames[16] have been investigated using CARS. In most of these studies temperature profiles alone were obtained but in certain cases concentrations have also been measured with CARS[17-19]. This paper presents our results of testing CARS as a combustion diagnostic in low luminosity flames (CH_4/air) and luminous flames (CH_4/N_2O) and the use of a computer analysis required for interpreting CARS spectra.

II. BACKGROUND

The first observation of the non-linear mixing process termed CARS was reported by Maker and Terhune[20] in 1965 and was only much later applied to combustion by Regnier and Taran[21] in 1973. Several review articles discuss

[11] *J.W. Nibler and G.V. Knighten, "Coherent Anti-Stokes Raman Spectroscopy," Raman Spectroscopy of Gases and Liquids, Topics in Current Physics, Vol. II, Springer-Verlag, New York, 1979.*

[12] *A.C. Eckbreth, R.J. Hall and J.A. Shirley, "Investigations of Coherent Anti-Stokes Raman Spectroscopy (CARS) for Combustion Diagnostics," AIAA Paper 79-0083, 17th Aerospace Sciences Meeting, New Orleans, La., Jan. 1979.*

[13] *A.C. Eckbreth, "CARS Thermometry in Practical Combustors," Combustion and Flame, Vol. 39, pp. 133-147, 1980.*

[14] *G.L. Switzer, L.P. Goss, W.M. Roquemore, R.P. Bradley, P.W. Schreiber, and W.B. Roh, "Application of CARS to Simulated Practical Combustion Systems," Journal of Energy, Vol. 4, pp. 209, 1980.*

[15] *I.A. Stenhouse, D.R. Williams, J.B. Cade, and M.P. Swords, "CARS in an Internal Combustion Engine," Applied Optics, Vol. 18, pp. 3819, 1979.*

[16] *L.E. Harris and M.E. McIlwain, "CARS Spectroscopy of Gun Propellant Flames," Technical Report ARLCD-TR-81007, 1981.*

[17] *A.C. Eckbreth and R.J. Hall, "CARS Concentration Sensitivity With and Without Nonresonant Background Suppression," Combustion Science and Technology, Vol. 25, pp. 175-192, 1981.*

[18] *M. Pealat, B. Attal, and J.P.E. Taran, "CARS Diagnostics of Combustion" AIAA 80-0282, 1980.*

[19] *L.A. Rahn, L.J. Zych, and P.L. Mattern, "Background-free CARS Studies of Carbon Monoxide in a Flame," Optical Communications, Vol. 39, pp.249, 1979.*

[20] *P.D. Maker and R.W. Terhune, "Study of Optical Effects Due to an Induced Polarization Third Order in the Electric Field Strength," Phys. Rev. Vol. 137, pp. A801-A818, 1965.*

[21] *P.R. Regnier and J.P.E. Taran, "On the Possibility of Measuring Gas Concentrations by Stimulated Anti-Stokes Scattering," Appl. Phys. Lett., Vol. 23, pp. 240-242, 1973.*

the CARS technique in detail[11,22,23] and thus only a brief description will be given here.

CARS is a four wave mixing process in which the interaction occurs through the third order non-linear susceptibility ($\chi^{(3)}$) which is associated with the third power of the applied electric field. For isotropic materials, gases and liquids, $\chi^{(3)}$ is the lowest order non-liner interaction. Two waves at a pump frequency ω_1 and one at a Stokes frequency ω_2 mix to produce a new coherent beam at the anti-Stokes frequency ω_3 which is equal to $2\omega_1-\omega_2$. This is visualized through the use of virtual states as is shown in Fig. 1a. This mixing process will occur at all frequencies but is greatly enhanced when $\omega_1 - \omega_2$ corresponds to a Raman active vibrational-rotational resonance (ω_{VR}). By scanning across ω_2 or using broad band radiation centered at ω_2, a spectrum can be obtained which contains information similar to a spontaneous Raman Stokes spectrum, Fig. 1b.

In addition to energy matching the incident laser beams to obtain a resonance condition, the momentum or phase matching condition $\Delta\vec{k} = 2\vec{k}_1 - \vec{k}_2 - \vec{k}_3 = 0$ is required. Here the momentum vector $\vec{k}$ is equal in magnitude to $n\omega/c$ where n is the frequency dependent index of refraction and c the speed of light. Three different geometrical configurations of vectors shown in Fig. 2 can meet this condition. In the most general crossed beam case two incident laser beams with momentum vectors $\vec{k}_1$ and $\vec{k}_2$ cross at a small angle θ. Phase matching can be made to work for samples in which the index of refraction varies with frequency. As an example phase matching can be obtained for the 992 cm^{-1} vibrational transition in benzene using $\theta \sim 1^{o}$. For gases the index of refraction varies little with frequency and $\theta \rightarrow 0$ resulting in a collinear arrangement of beams, Fig. 2b. This alignment has the advantage of a long interaction length thus producing large CARS signals (CARS depends on the square of the interaction length).[23] Disadvantages of this configuration are poor spatial resolution and unwanted CARS signal contributions. In the majority of cases the temperature of a flame is determined from the information in the CARS signal for N_2. Here contributions from room air outside of the flame can dominate the CARS signal if careful shielding of the overlapped laser beams is not used. A method of circumventing these problems and still meeting the phase matching requirement has been introduced by Eckbreth[24] and is termed BOXCARS. In this case the pump laser beam at ω_1 is split into two components shown in Fig. 2c and the resulting vector diagram for $\Delta\vec{k} = 0$ forms the shape of a box. High spatial resolution can be obtained with this method. Both collinear and BOXCARS

---

[22] *S.A. Akhmanov and N.I. Koroteev, "Spectroscopy of Light Scattering and Nonlinear Optics. Nonlinear-Optical Methods of Active Spectroscopy of Raman and Rayleigh Scattering,"* Sov. Phys. Usp. *Vol. 20, pp. 899-936, 1977.*

[23] *W.M. Tolles, J.W. Nibler, J.R. MacDonald, and A.B. Harvey, "A Review of the Theory and Application of Coherent Anti-Stokes Raman Spectroscopy (CARS),"* Applied Spectroscopy. *Vol. 31, pp. 253-271, 1977.*

[24] *A.C. Eckbreth, "BOXCARS: Crossed-Beam Phase-Matched CARS Generation in Gases,"* Appl. Phys. Lett. *Vol. 32, pp. 421-423, 1978.*

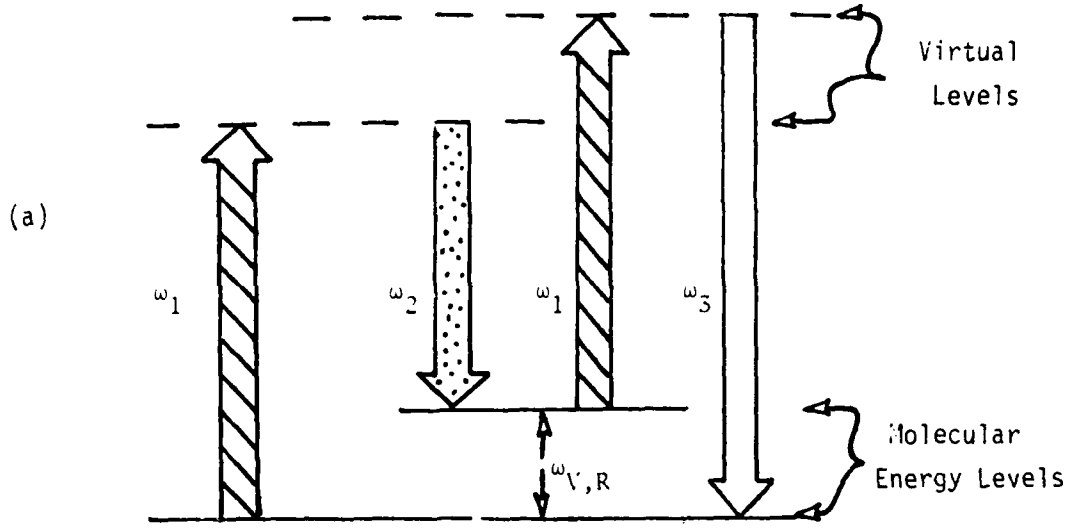

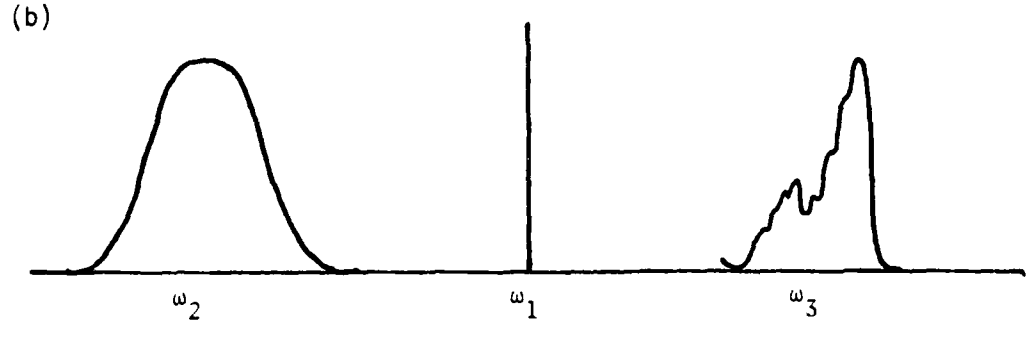

Figure 1. (a) Representative energy level diagram where ω_1 and ω_2 are laser frequencies, ω_3 is the CARS signal produced and $\omega_{V,R}$ is an allowed molecular vibrational or rotational energy spacing. (b) Representative frequency spectrum when using broadband laser radiation centered at ω_2.

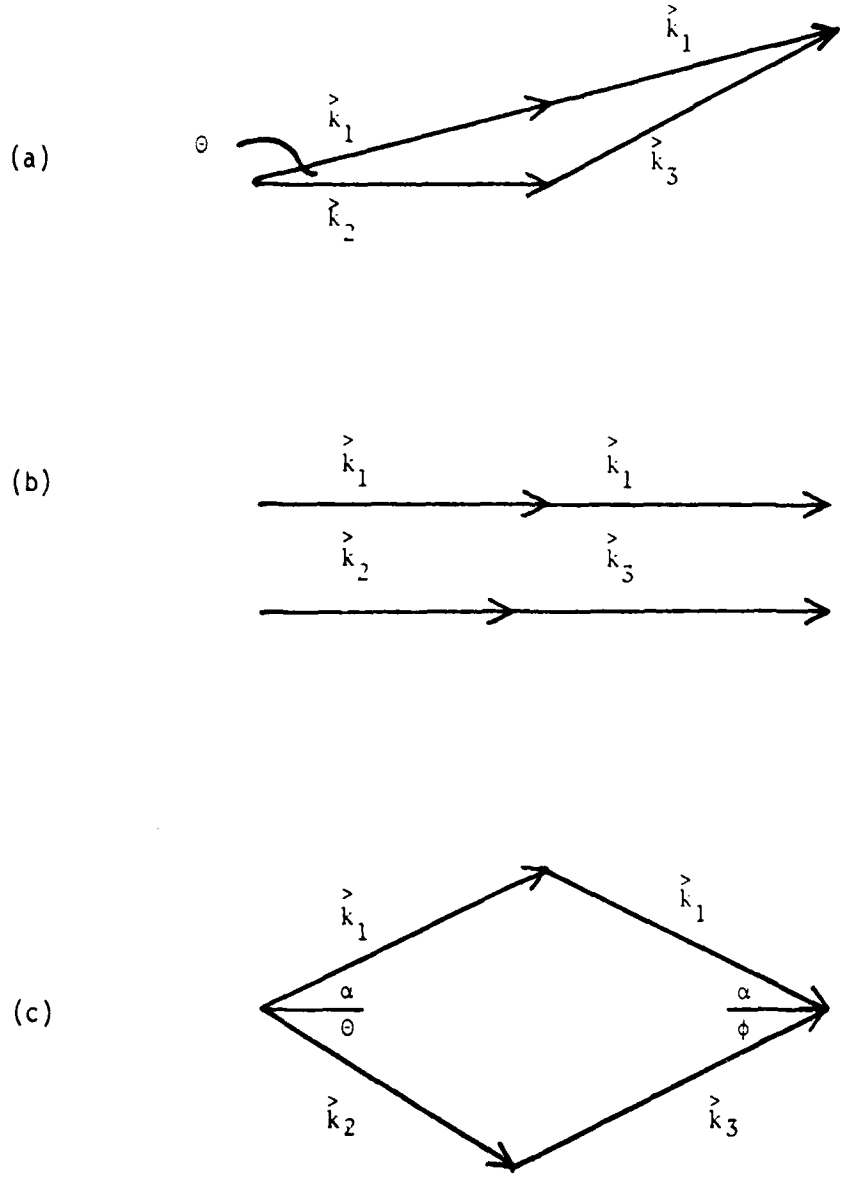

Figure 2. Three of the most common geometries used for phase matching ($\Delta \vec{k} = 0$) of the laser beams (a) crossed beams, (b) collinear beams and (c) BOXCARS, where the ω_1 laser beam is split into two components. This geometry can result in much better spatial resolution than (a) or (b).

configurations were used for the experimental results presented in this paper. A variation of BOXCARS called folded BOXCARS has also recently been used in studies of rotational CARS[25]. In this case the $\vec{k}_1$ and $\vec{k}_2$ vectors are not in the same plane and thus the ω_3 CARS beam appears in a place well separated from both ω_1 beams. This configuration was not employed in this investigation.

The polarization of the incident laser beams must also be oriented in certain directions to produce substantial CARS signals. Generally the polarizations of the ω_1 and ω_2 beams are aligned to produce the most intense CARS signals[26] In special circumstances, such as suppression of the non-resonant susceptibility which can mix with the resonant contribution,[17,19,27] other polarization techniques are used but they will not be discussed here. For this work only the configuration where all laser polarizations are aligned in the same plane was used.

III. EXPERIMENTAL

A schematic diagram of the CARS experimental apparatus is shown on Fig. 3. A commercial Nd:YAG Quantel Model 481C laser was used as the excitation source. This laser produces approximately 500 mj per pulse of energy at 532 nm when operated at 10 Hz. It has a pulse length of about 15 ns and a linewidth of ~0.2 cm^{-1}. The ω_1 beam, vertically polarized,[28] is routed by dichroic mirrors M1-M6 which have maximum reflectance at 532 nm and maximum transmission at 1064 nm thus allowing separation of the fundamental from the experiment. The fundamental is terminated with a beam block (not shown). BS1 is a 50/50 beamsplitter which splits off half of the ω_1 beam for pumping the dye laser. A Quantel Model TDL III dye laser was used to supply the light at frequency ω_2[28]. This dye laser, as obtained from the manufacturer, operates at narrow linewidths which are obtained with a tuning mechanism consisting of a grazing angle of incidence grating and return mirror. To create broadband radiation from this dye laser the optical path from the grating and return mirror was blocked. In addition a broad band high reflectance mirror was placed just past the grating which returned some of the zeroth order grating light back to the oscillator dye cell. Adjustment of this mirror allowed the dye laser to lase essentially over the complete dye gain curve.

---

[25] *J.A. Shirley, R.J. Hall, and A.C. Eckbreth, "Folded BOXCARS for Rotational Raman Studies," Optics Letters, Vol. 5, 380-382, 1980.*

[26] *M.D Levenson and N. Bloembergen, "Dispersion of the Nonlinear Optical Susceptibility Tensor in Centrosymmetric Media," Phys. Rev. B Vol. 10, pp. 4447-4463, 1974.*

[27] *R.L. Farrow, R.E. Mitchell, L.A. Rahn, and P.L. Mattern, "Crossed-Beam Background-Free CARS Measurements in a Methane Diffusion Flame," AIAA-81-0182, 1981.*

[28] *Polarization of ω_1 can be made either horizontal of vertical by orientation of the frequency doubling crystal. To obtain essentially one polarization in the dye laser a Glan-air prism can be inserted in the oscillator cavity and thus the polarization can be changed by orientation of this prism.*

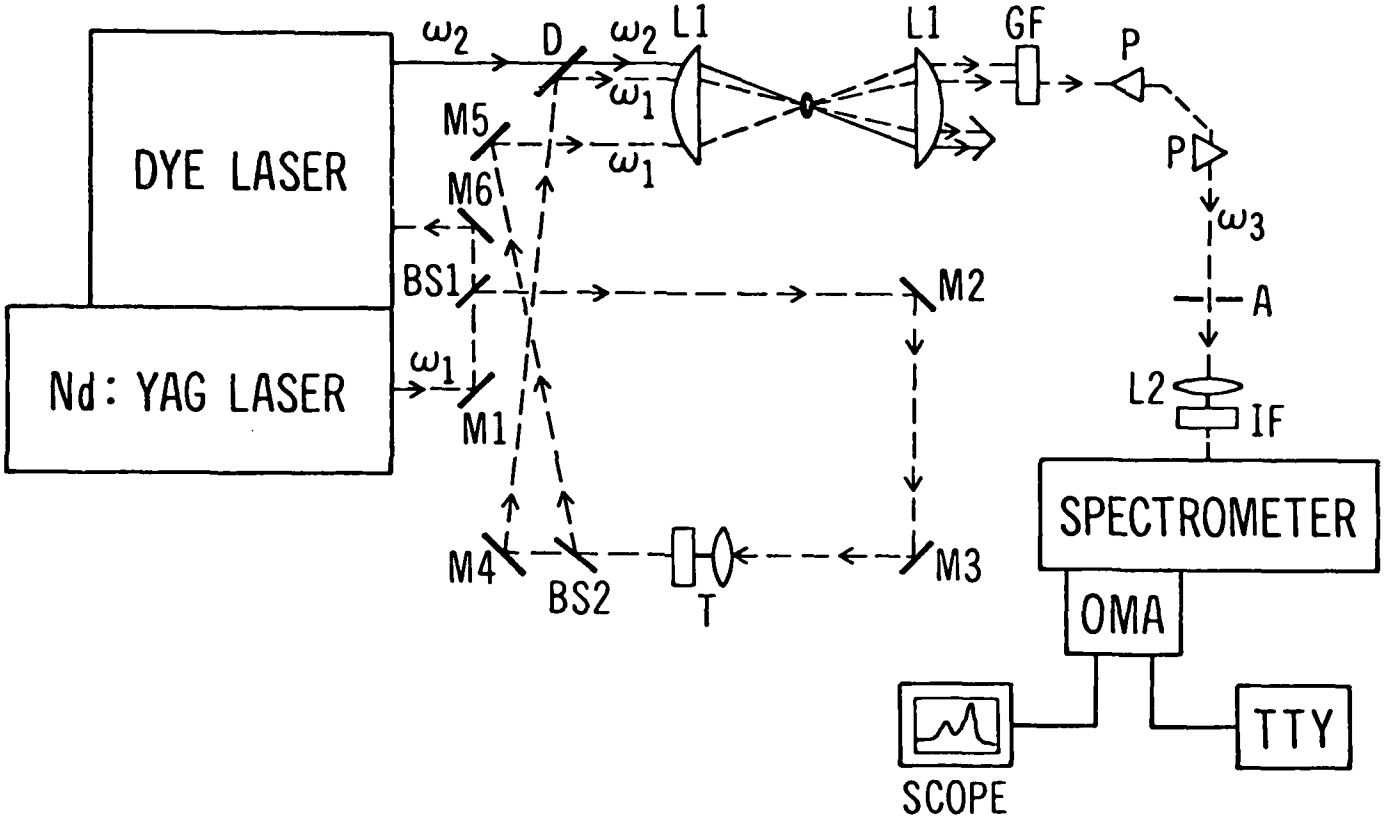

Figure 3. A Diagram of the Experimental Apparatus.

Since this dye laser consists of one oscillator and three amplifiers a substantial optical delay line (4m) was required to temporally match the ω_2 radiation with that of ω_1 at the point of intersection of the beams. This optical delay line is represented in Fig. 3 from BS1 through M4. BS2 is another 50/50 beamsplitter which splits the ω_1 beam for the BOXCARS configuration. D is a dichroic mirror which reflects the ω_1 (532 nm) radiation and allows most of the ω_2 radiation to pass through. When producing a CARS signal for N_2, ω_2 is centered at ~606 nm, 680 nm for H_2, and D allows greater than 70% transmission at these wavelengths. This transmission is highly dependent on the angle of incidence of the ω_2 radiation.

L1 and L2 provide the focussing, intersection and recollimation of the ω_1 and ω_2 beams. These lenses are 7.6 cm in diameter with a 30.5 cm focal length. At the intersection point it is desirable for the beams to waist and have similar diameters for efficient CARS signal generation. A telescope, T, was used for this purpose. Several stages of filtering are used to eliminate the ω_1 and ω_2 radiation from ω_3. Glass absorption filters, GF, are used to absorb > 95% of the ω_1 and ω_2 radiation while passing ~50% of the ω_3 signal. Spatial separation of the remaining beams is accomplished by using two extra dense flint prisms, P. Later these two prisms were replaced by a rutile prism. The ω_3 beam then passes through an aperture A and is focussed into a 0.25 m spectrometer by L2 which has a 7.6 cm focal length. An interference filter, IF, is placed just in front of the spectrometer entrance to remove any stray ω_1 and ω_2 light. This filter blocks ~99 % of 532 nm radiation and passes ~ 85% of the ω_3 radiation. The spectrometer was positioned such that the entrance slits, 100 μ, were horizontal, that is, parallel to the plane of the laser beams. This arrangement eliminated a potential problem of not capturing all of the requisite spectrum since the spatial dispersion, from the prisms, disperses the light along the long dimension of the entrance slit (1 cm). A silicon intensified target vidicon tube, PAR Corp. optical multichannel analyzer (OMAI) Model 1205D, was used to detect the dispersed light of the spectrometer. Either of two gratings, 1180 or 2360 grooves/mm, can be switch selected. Using a grating of 1180 grooves/mm one finds approximately 40 nm of radiation can be observed at one time. This radiation is dispersed on 500 memory channels which gives a resolution of 0.08 nm per channel.

Two memories of the OMA allow summation of scans to obtain data from one or more laser pulses and also noise subtraction. In practice the CARS signal and background noise are recorded in memory A, then the CARS signal is removed by blocking the ω_2 beam and this background noise signal is recorded in memory B. Subtraction of B from A results in a relatively noise free CARS signal. The contents of the OMA can be observed on a display scope or digitally outputted on a teletype and paper tape.

To generate N_2 CARS signals the dye laser was centered at ω_2 ~606 nm using one part Rhodamine 640 to four parts Rhodamine 610 by volume in a methanol solvent at concentrations of ~ 10^{-4} moles/liter. For H_2 CARS signals, ω_2 is centered at 680 nm. Oxazine 720 dye in methanol at concentrations of ~ 5×10^{-3} moles/liter produced the desired wavelengths. The full width half maximum (FWHM) bandwidth for the dye mixtures was about 5 nm. A photograph of the output from the OMA display scope showing the broadband output is shown in Figs. 4a and b. An easy method of determining where the dye laser is centered can be accomplished by operating the TDL III

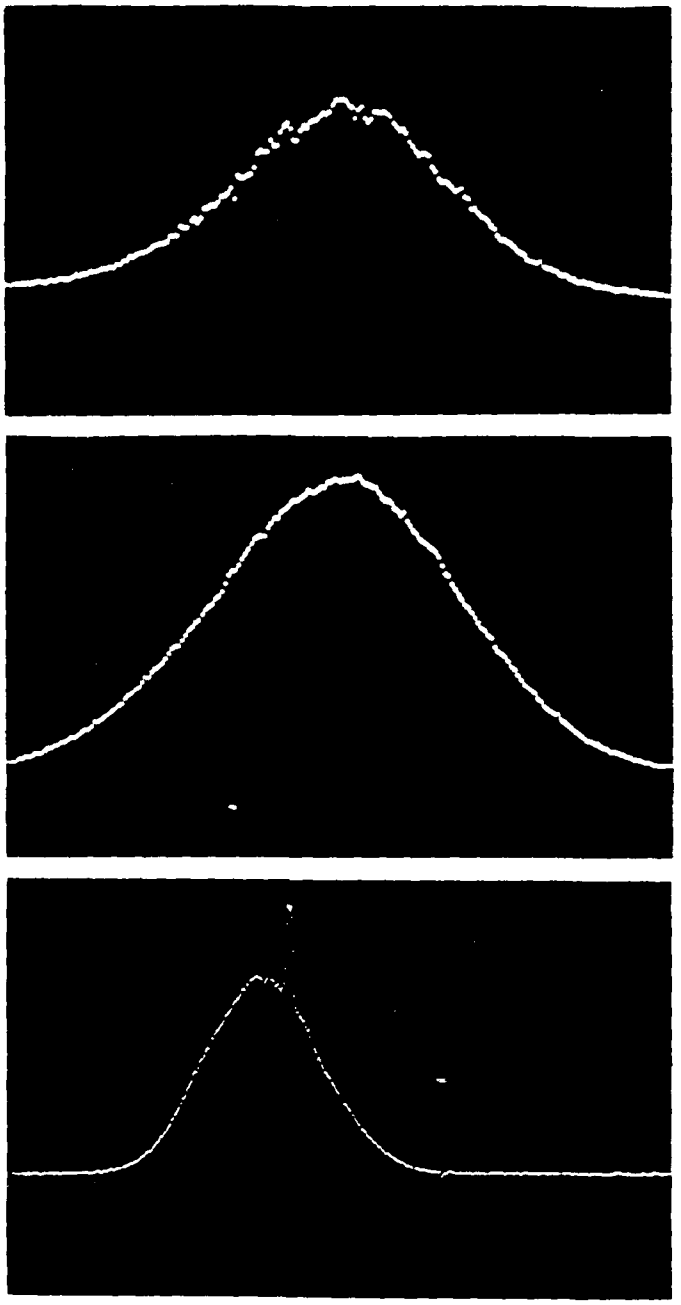

Figure 4. Frequency spectra of the dye laser. (a) Broadband dye laser output from a single laser shot. The peak is centered at 631 nm with a FWHM of about 110 cm^{-1}. (b) Same conditions as in (a) except 16 laser shots were accumulated. (c) The dye laser was operated such that a broadband and narrowband output was produced simultaneously for the purpose of checking the center frequency. Here the narrowband output is 633 nm as indicated by the calibrated wavelength dial of the dye laser.

dye laser in the broad and narrow band modes simultaneously (that is, allow the dye oscillator light from the grating to return to the oscillator cell as well as the light returned from the broad band reflector mirror). The dye laser output for this configuration is shown in Fig. 4c.

A porous plug burner made from sintered copper shown in Fig. 5 was used to support the various flames used in this study. The sintered plug diameter is 2.8 cm and is edge cooled by water flowing through a copper coil soldered to the burner case. All of these studies were conducted at atmospheric pressure.

The spatial resolution of the CARS experiment in the vertical direction (a plane parallel to the flow of burner gases) is given to a good approximation by the product of the focal length of the focussing lens (30.5 cm) and the divergence of the laser beam $\leq 0.5 \times 10^{-3}$ radians. This gives a vertical resolution of about 150 μ. The resolution in the horizontal direction (a plane perpendicular to the flow of burner gases) varies depending on whether collinear or BOXCARS geometry is used. Furthermore for BOXCARS geometry the resolution depends on the crossing angle of the laser beams. For the collinear case, assuming no room air contributions arise, the horizontal resolution is about 6 cm. The BOXCARS configuration is capable of producing much better horizontal resolution. Although the resolution was not investigated in detail here, Eckbreth[24] measured a resolution of 4 mm (the spatial extent where the CARS signal grew from 10% to 90%) for a geometrical arrangement similar to our investigations. Higher spatial resolution was not attempted or necessary for the results reported here; however, spatial resolutions covering volumes of less than 1 mm^3 should be easily attainable. If sufficient data can be obtained in a single laser pulse the temporal resolution is 10^{-8} seconds.

IV. ANALYSIS OF CARS SPECTRA

The fitting routine used to the reduce the experimental CARS spectra is a modification of a least squares program which has been previously used to extract spectroscopic constants from measured transition frequencies.[29] The program uses the equation

$$I_o\ (\omega_1^o, \omega_2^o, \nu_o) = \int d\omega \left|\chi\ (\omega)\right|^2 \exp\ [\ -\ \frac{AB}{A+B}\ (\omega\ -\ \omega_o)^2]$$

$$\int\ d\omega_3\ S\ (\nu_o, \omega_3)\ \exp\ [\ -\ A\ (\omega_3\ -\ \omega\ -\ \omega_1^o\ )^2\ ] \qquad (1)$$

to fit the N_2 and H_2 CARS spectra obtained from laboratory flames. In Eq. 1, I_o is the observed CARS signal intensity, ω_1^o and ω_2^o are the center frequencies of the pump and Stokes laser profiles respectively and $\omega_o = \omega_1^o - \omega_2^o$, ν_o is

---

[29] *A.J. Kotlar, R.W., Field, J.I. Steinfeld and J.A. Coxon, "Analysis of Perturbations in the $A^2\pi$ - $X^2\Sigma^+$ Red System of CN,"* Journal of Molecular Spectroscopy, *Vol. 80, p. 86-108, 1980.*

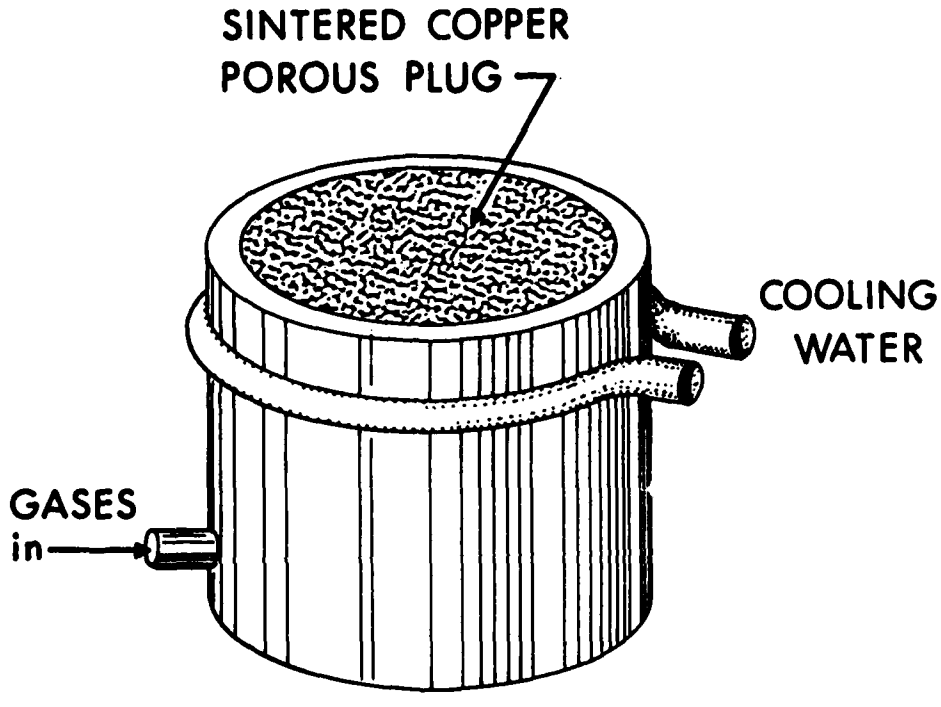

Figure 5. An edge cooled porous plug burner used to support the flames investigated in this report.

the center frequency of the detector slit function S, and A and B are related to the widths of the ω_1 and ω_2 laser profiles, which are assumed to be Gaussian. $A = 4 \ln 2 / (\Delta\omega_1)^2$ and $B = 4 \ln 2 / (\Delta\omega_2)^2$ where $\Delta\omega_1$ and $\Delta\omega_2$ are the laser widths (FWHM). A more detailed description of the CARS equation and commonly used slit width functions can be found in Ref. 30. The computer program performs a multiparameter fitting to obtain a best fit to the data. The program also calculates the variance/covariance matrix from which the standard deviation, as statistically determined from the fit, is evaluated.

For nitrogen spectra, typically six parameters were varied in the fit. These included the temperature, a scaling factor for the spectrum which corresponds to the number density, a baseline, the slit width, the resolution of the detector (Å/ channel for the OMA) and a reference wavelength to tie the spectrum to an absolute scale.

The spectrum for hydrogen is much better resolved than for the nitrogen case; thus the pressure broadened rotational linewidth was also adjusted in the fit. For some of the hydrogen experiments (CH_4 diffusion flame and the rich CH_4/N_2O premixed flame) a large background is present due to collinear phase matching and low relative concentrations of H_2. As will be discussed later, this background feature is determined by the non-resonant susceptibilities and the position and shape of the dye laser profile. To properly account for this spectral feature in the computer fit four additional parameters are required. These parameters are the non-resonant susceptibility of the flame gases, the non-resonant susceptibility of room air, the center frequency and width of the dye laser profile. These parameters can be experimentally determined or found in the literature, however they were not constrained to one value, but rather allowed to be changed by the least squares fitting procedure.

The spectroscopic constants for nitrogen were taken from Huber and Herzberg[31]. The spectrum was calculated for all O, Q and S transitions for vibrational levels v" = 0 to 4 and rotational levels J" = 0 to 60. For the region of the spectrum corresponding to the range of the experimental data, transitions from 2269 to 2350 cm^{-1} must be included in the fitting program. This gives 153 transitions from (3,2) Q(13) to (1,0) S(1). The spectroscopic constants for hydrogen were also taken from Ref. 31, where the higher order constants are from Fink et al.[32] Reference is also made to more recent values

---

[30] *A.J. Kotlar and J.A. Vanderhoff, "A Model for the Interpretation of CARS Experimental Profiles," accepted for publication in Applied Spectroscopy. "Interpretation and Least Squares Fitting of CARS Experimental Profiles," BRL report in preparation.*

[31] *K.P. Huber and G. Herzberg, "Molecular Spectra and Molecular Structure IV. Constants of Diatomic Molecules," Van Nostrand Reinhold Company, New York 1979.*

[32] *U. Fink, T.A. Wiggins and D.H. Rank, "Frequency and Intensity Measurements on the Quadrupole Spectrum of Molecular Hydrogen," J. Mol. Spectrosc. Vol. 18, p. 384, 1965.*

by the same workers[33]. We found that the earlier values[32], that is those actually listed in Huber and Herzberg, gave transition frequencies which better agreed with those we observed in our experiments, and these were used to generate the table of transitions used in the program. For the hydrogen spectrum corresponding to the range of experimental data 3940 to 4200 cm^{-1}, it was only necessary to include vibrational levels v" = 0 and 1, and rotational levels J" = 0 to 8. Within this range only the (1,0) Q branch is present giving 9 transitions from Q(0) to Q(8).

V. RESULTS

Initially collinear CARS was employed to survey qualitatively the shape and characteristics of various CARS spectra. No temperature fitting was attempted at this point. Fig. 6a shows a room air N_2 CARS signal which has a relatively symmetric shape with a FWHM resolution of about 6 cm^{-1}. Figs. 6b and 6c show the N_2 CARS signal obtained in a slightly rich CH_4/N_2O flame without and with shields, respectively. The shields were hollow tubes placed between (see Fig. 3) the focussing lens and the burner and between the burner and the recollimating lens. Helium gas was flowed through these tubes to displace the room air. The effect of shielding is readily apparent from the differences observed in Figs. 6b and 6c. Fig. 6c has a distinct second peak, a hot band denoting a higher N_2 temperature. Since these shields proved troublesome, it was necessary to go to the BOXCARS configuration when room air contributions could be present (i.e. the study of N_2 or O_2 molecules).

The signal strength for BOXCARS is less than for collinear geometry due to a smaller interaction length; thus we chose to first look at a near stoichiometric CH_4/air flame where the N_2 density is larger than for a CH_4/N_2O flame. Figures 7a,b show BOXCARS spectra for N_2 taken at two positions perpendicular to the plane of the burner surface. The temperature values with standard deviations are listed in Table 1. A crossing angle (2 α) of 6° was used. The 2360 groove/mm grating gave a FWHM resolution of 3.8 cm^{-1}. This resolution is sensitive to the focussing of the lens L2 and is determined from the CARS computer fitting program by best fits to the data especially on room air where the temperature is precisely known. The resulting temperature profile is suggestive of several phenomena associated with the flame. First, at the 1 mm position the temperature is much lower than the other (higher) positions indicating that we are sampling somewhere in the reaction zone, a place prior to complete combustion. Second, the highest temperature measured is 1790K whereas the adiabatic flame temperature for a stoichiometric CH_4/air flame at atmospheric pressure is calculated from the NASA-Lewis thermochemical equilibrium code[34] to be 2226K. A substantial amount of heat is thus being extracted from the flame by the burner head[35]. Third, the burnt gas region of

[33] *J.V. Flotz, D.H. Rank and T.A. Wiggins, "Determinations of Some Hydrogen Molecular Constants", J. Mol. Spectrosc. Vol. 21, p. 203, 1966.*

[34] *R.A. Svehla and B.J. McBride, "Fortran IV Computer Program for Calculation of Thermodynamic and Transport Properties of Complex Chemical Systems", NASA TN D-7056 (1973).*

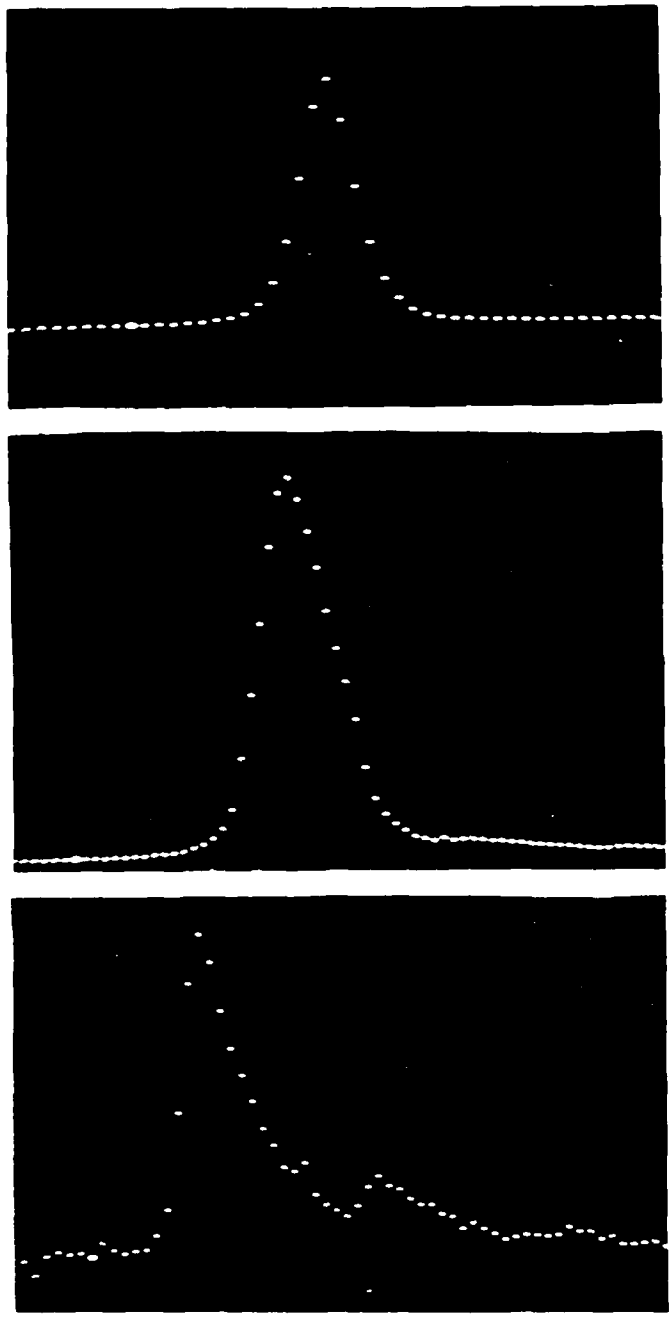

Figure 6. Photographs of the N_2 CARS signal obtained in room air and a flame environment using collinear geometry. (a) room air, (b) a rich CH_4/N_2O flame without shielding from air contributions, and (c) the same flame as in (b) except shields were used to eliminate room air contributions.

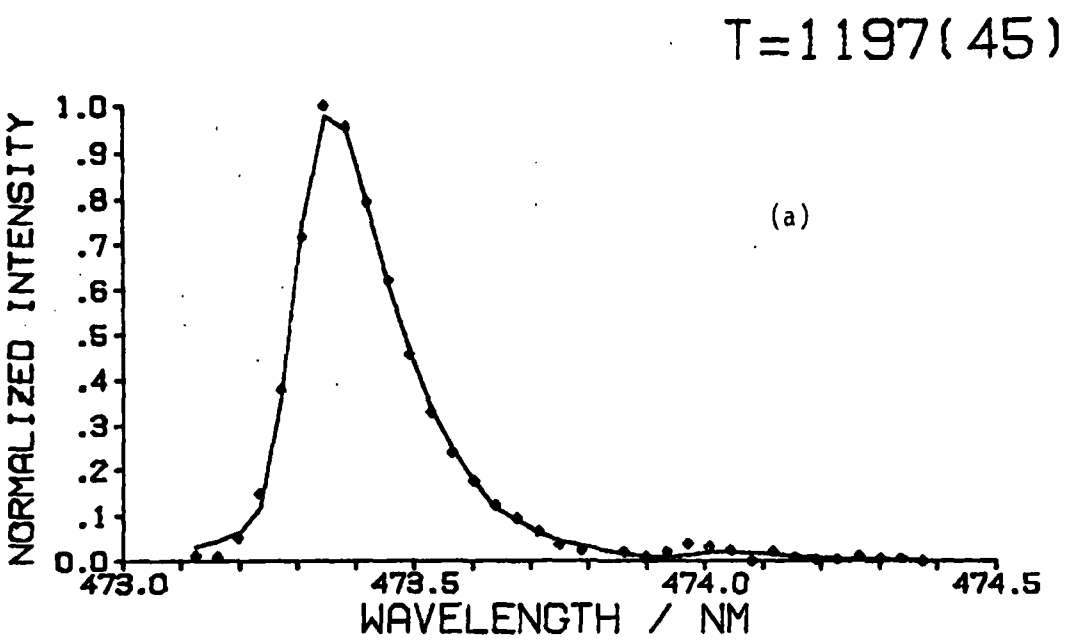

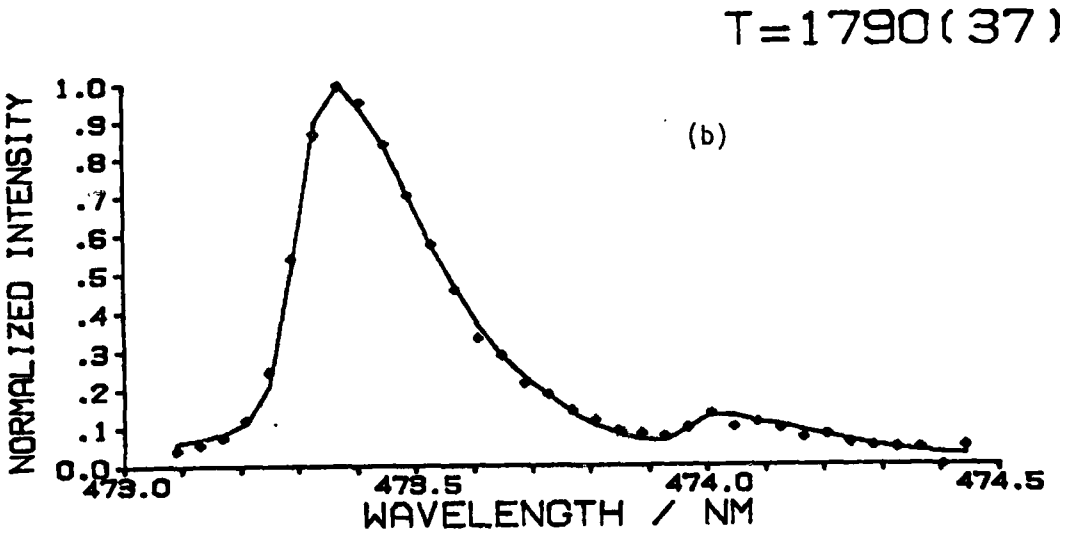

Figure 7a,b. N_2 CARS spectra obtained in a near stoichiometric CH_4/air flame using BOXCARS geometry and a 2360 groove/mm grating. The experimental data are shown as points and the solid line is the least squares computer fit. The temperature resulting from the fit and the standard deviation are given on each spectrum. This holds for all subsequent CARS spectra.

Height (mm)	Temperature (K)
1	1197±45
4	1790±37
9	1645±51
14	1553±39
19	1687±44

Table 1. Vertical temperature profile values obtained in a near stoichiometric CH_4/air flame using BOXCARS geometry with a crossing angle of 6° (2α). A 2360 groove/mm grating was used giving a resolution of about 4 cm^{-1} (FWHM). The least squares computer fits which are tabulated in the three tables have the resolution as a variable parameter to be determined by the best fit thus the resolutions quoted here are average values which may vary as much as ±.3 cm^{-1} from run to run. The number of laser shots for each temperature determination varied from 5 to 50 shots.

the flame (4 mm through 19 mm) does not show either a constant temperature or a slow fall off but instead a decrease followed by an increase in temperature. This behavior is indicative of a second flame zone which could result if the flame is slightly rich and a secondary zone forms from combustion with entrained air.

The next set of CARS measurements were made on a near stoichiometric CH_4/N_2O flame using BOXCARS geometry with a crossing angle of 3.9°. A vertical and radial temperature profile is illustrated on Figures 8a and 8b with values listed in Table 2. Each data point was a sum of 300 laser pulses and representative CARS spectra for two of these data points are shown on Fig. 9a and 9b. Here a 1180 groove/mm grating was used resulting in the signal being displayed on half as many OMA channels as the data of Figs. 7 and 11. With the exception of the positions higher than 10 mm and at the edges of the burner the temperatures agree within the constraints of the standard deviation (see Table 2). Above 10 mm the flame is cooled by heat loss to the surrounding air. At the edges of the burner where steep gradients are present, it is not surprising to find differences in the temperature results. Another vertical and radial temperature profile in a near stoichiometric CH_4/N_2O flame was obtained using the 2360 groove/mm grating. The profiles are shown in Figs. 10a and 10b, and the values are given in Table 3. Representative CARS spectra for two of these data points are shown in Figs. 11a and 11b.

It is interesting to compare the results of Figs. 8 and 10. These data were obtained on different days; hence the equipment and flame were subject to the routine tasks of turn-off-turn-on and alignment between data sets. The flame temperatures measured from 0 - 10 mm in the vertical direction and close to the centerline radially exhibit excellent agreement between data sets. Above 10 mm and close to the edge radially the temperatures differ substantially. This effect is most likely caused by the chimney which captures the burnt gases of the flame. The closer the chimney is placed to the burner the more the flame contracts to the centerline of the burner as a function of vertical height above the burner surface. Although the airflow up the chimney provides for stabilization of the flame against fluctuating room air currents it also changes the geometry of the flame near the edges of the burner and causes greater cooling high above the burner surface. The data for Fig. 10b were taken with the chimney closer to the burner resulting in the steeper gradients observed.

By comparing the standard deviations of the temperatures shown in Tables 2 and 3 one observes that the deviation is larger for the lower resolution data which is expected. The resolution obtained with the 1180 groove/mm grating (~12 cm^{-1}) is about the lowest resolution that can be used and still obtain reasonable precision at flame temperature (~2000K) for N_2 CARS spectra. At lower temperatures higher resolution is necessary since smaller contributions from the N_2 hot band occur and thus the temperature must be determined predominantly from the shape of the single peak.

[35] *This effect has been observed in our laboratory whenever using porous plug burners in spontaneous Raman and fluorescence studies. See for example W.R. Anderson, L.J. Decker, and A.J. Kotlar, "Temperature Profile of a Stoichiometric CH_4/N_2O Flame from Laser Excited Fluorescence Measurements on OH," accepted for publication in Combustion and Flame.*

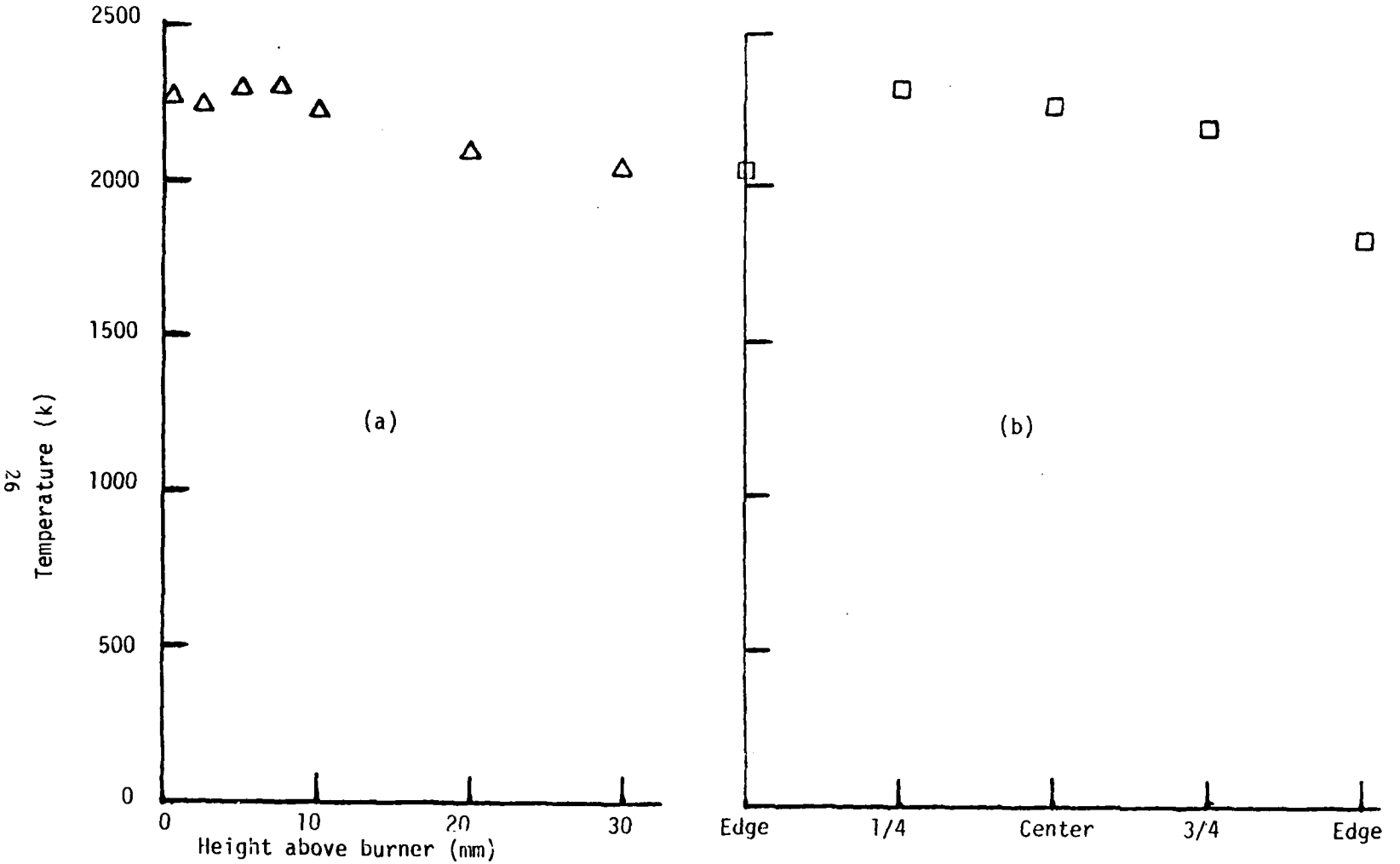

Figure 8. N_2 CARS temperature profiles obtained in a near-stoichiometric CH_4/N_2O flame; (a) vertical profile (b) radial profile.

Height (mm)	Radial Position	Temperature (K)
0.5	centerline	2271±73
2.5	centerline	2249±38
5.0	centerline	2304±50
7.5	centerline	2309±37
10.0	centerline	2234±40
20.0	centerline	2101±4
30.0	centerline	2068±19
5.0	edge	2083±45
5.0	1/4	2333±90
5.0	centerline	2278±77
5.0	3/4	2209±39
5.0	edge	1841±36

Table 2. Vertical and radial temperature profile values obtained in a near-stoichiometric CH_4/N_2O flame using BOXCARS geometry with a crossing angle of 3.9°. A 1180 groove/mm grating was used giving a resolution of 12 cm^{-1}. An accumulation of 300 laser shots per temperature point was used.

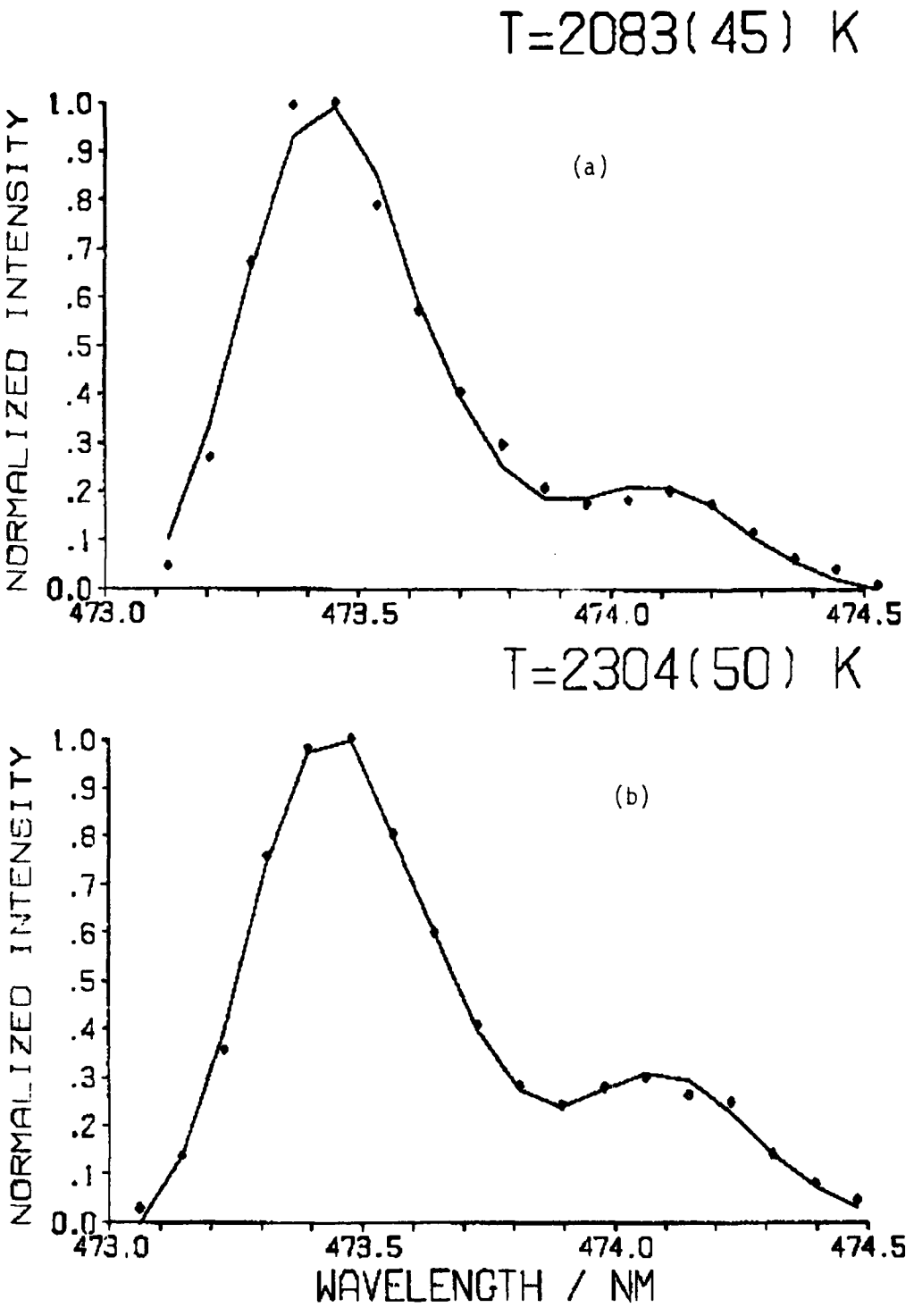

Figure 9a,b. Two representative N_2 CARS spectra for two of the data points of Fig. 8. BOXCARS geometry and a 1180 groove/mm grating was used.

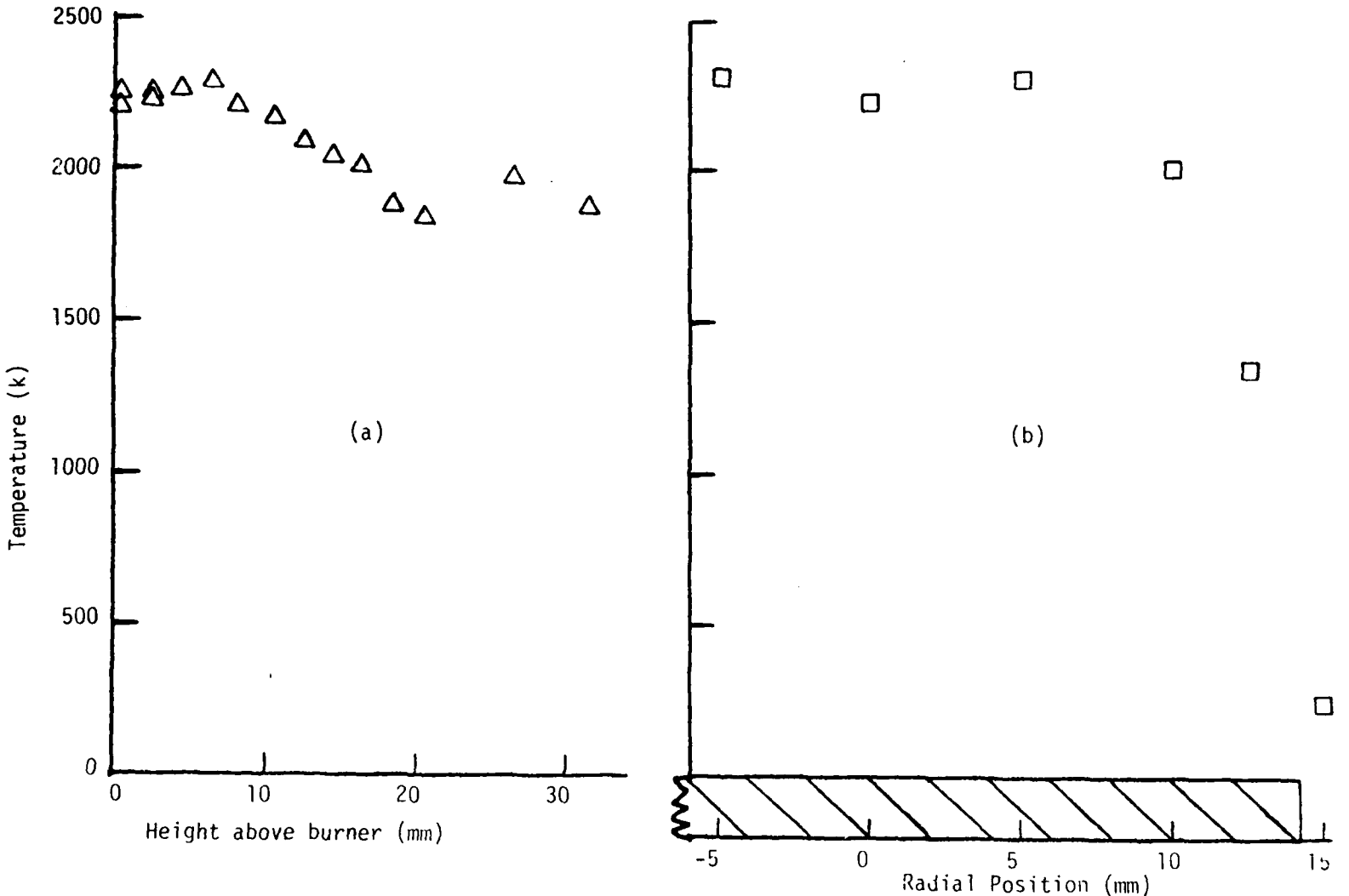

Figure 10. N_2 CARS temperature profiles obtained in a near-stoichiometric CH_4/H_2O flame; (a) vertical profile (b) radial profile.

Height (mm)	Radial Position (mm)	Temperature (K)
0.5	centerline	2270±10
0.5	centerline	2278±30
0.5	centerline	2226±37
2.5	centerline	2234±35
2.5	centerline	2250±40
4.5	centerline	2271±38
6.5	centerline	2302±29
8.5	centerline	2208±28
10.5	centerline	2181±52
12.5	centerline	2096±23
14.5	centerline	2040±23
16.5	centerline	2016±24
18.5	centerline	1892±22
20.5	centerline	1855±54
26.5	centerline	1985±40
31.5	centerline	1880±26
2.5	-5	2320±45
2.5	+5	2315±40
2.5	+10	2017±24
2.5	12.5	1343±19
2.5	15	227±30

Table 3. Vertical and radial temperature profile values obtained in a near-stoichiometric CH_4/N_2O flame using BOXCARS geometry with a crossing angle of 3.9°. The 2360 groove/mm grating gave an overall resolution of 4 cm^{-1}. An accumulation of 650 laser shots were used per temperature point.

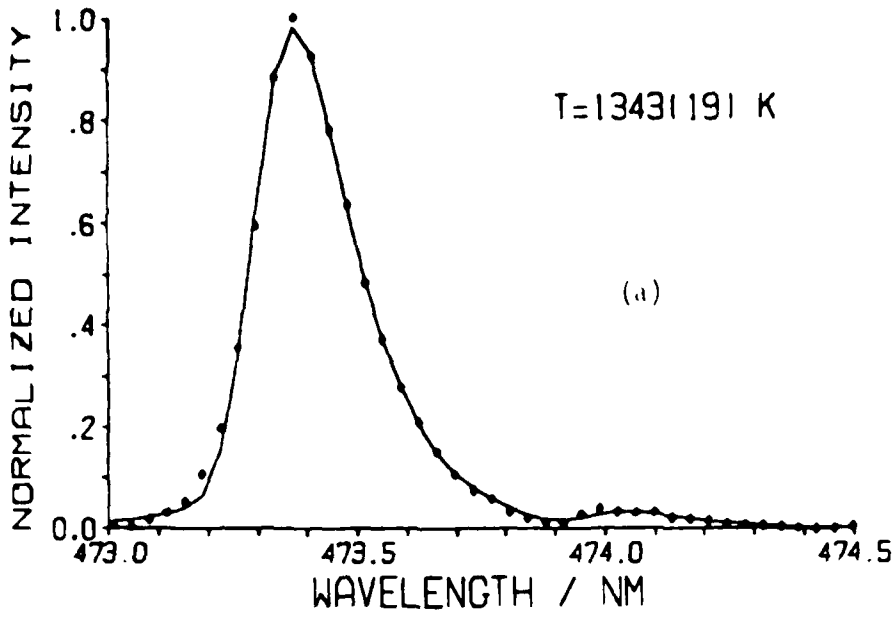

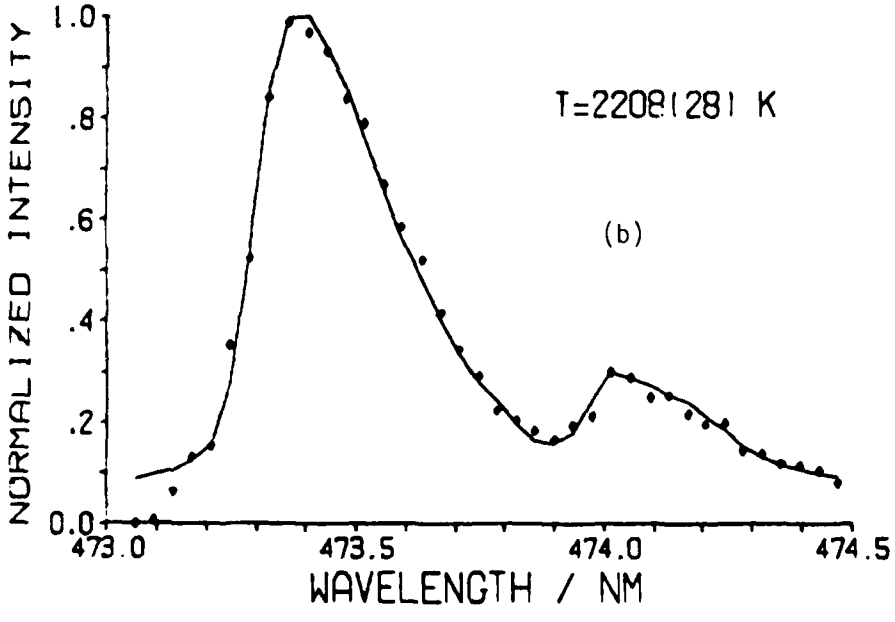

Figure 11a,b. Two representative N_2 CARS spectra for two of the data points of Fig. 10. BOXCARS geometry was used and a 2360 groove/mm grating.

Temperature determinations were also made from CARS spectra of the H_2 molecule in a flame environment. H_2 has a well separated rotational spectrum due to its small moment of inertia (H_2 has a rotational constant of 60.8 cm^{-1} while N_2 is 2.01 cm^{-1})[36] and thus the CARS spectrum of H_2 shows well resolved rotational structure within the 0 to 1 vibrational Q-branch transition. Figs. 12a-d illustrate H_2 CARS spectra obtained in (a) pure H_2 at room temperature, (b) a H_2 diffusion flame, (c) a CH_4 diffusion flame and (d) a rich CH_4/N_2O premixed flame. In order to generate the spectrum of Fig. 12a pure H_2 was flowed unignited through the porous plug burner and measurements were made 4 mm above the burner surface using BOXCARS geometry with a crossing angle of 3.9°. The resulting H_2 CARS signal was easily observable with the eye and had to be attenuated by 99% before entering the detector. The generated spectrum is from a single shot. The largest peak at this temperature is Q(1), i.e. the J = 1 rotational line of the Q branch. Q(0) appears as a shoulder to the left of Q(1), and Q(2) and Q(3) are also observable. The computer model code for H_2 was constrained to fit this data with the room temperature value of 290K. In Fig. 12b the H_2 flowing through the porous plug burner was ignited producing a H_2/air diffusion flame from which a temperature determination was made at a position 40 mm above surface[37]. This position appeared visually to be the hottest part of the diffusion flame. Here the CARS signal was substantially smaller and Fig. 12b represents 160 laser shots with no attenuation in the CARS signal beam. BOXCARS geometry was again used with the 3.9° crossing angle. At this hotter temperature the higher rotational lines Q(4) through Q(7) are observable. Higher rotational lines would also be observed if the dye laser had a broader bandwidth or shifted to higher wavelengths. A temperature of 2406±58K was obtained from the least squares computer fit. This experimentally determined temperature is higher than the adiabatic flame temperature, 2382K, computed for a stoichiometric H_2/air flame from the NASA-Lewis code.[34] Since the investigation of H_2 CARS signals in flame environments was of a survey nature we did not do any detailed investigation of this difference. Nonetheless, possible explanations for this difference are that the center frequency of the dye laser shifted from the calibrated value, or the linewidth and lineshape for H_2 are different from those used in the computer program. In the computer program linewidths (Lorentzian) for N_2 were fixed at 0.1 cm^{-1}, for H_2 varied from 0.09 to 0.15 cm^{-1}. For H_2 a Voigt profile was used for the lineshapes. At these temperatures (~2000K) H_2 falls into the Dicke narrowing regime and the chosen lineshape may not be strictly valid. A discussion of the variation of H_2 linewidth with pressure and temperature can be found in Ref. 38.

---

[36] G. Herzberg, Spectra of Diatomic Molecules, (Van Nostrand Reinhold, New York, 1950).

[37] *It was stated earlier that the burner head cooled the flame substantially. This holds true only for premixed flames where the flame is stabilized on the burner head. In the diffusion flames where room air is the oxidant, the reaction zone is cone shaped due to the way the air mixes with the fuel. Around the tip of the cone (40 mm) where the measurement was made there is negligible heat loss to the burner.*

[38] J.A. Shirley, A.C. Eckbreth, and R.J. Hall, "Investigation of the Feasibility of CARS Measurements in Scramjet Combustion," UTRC Report R79-954390-8, 1979.

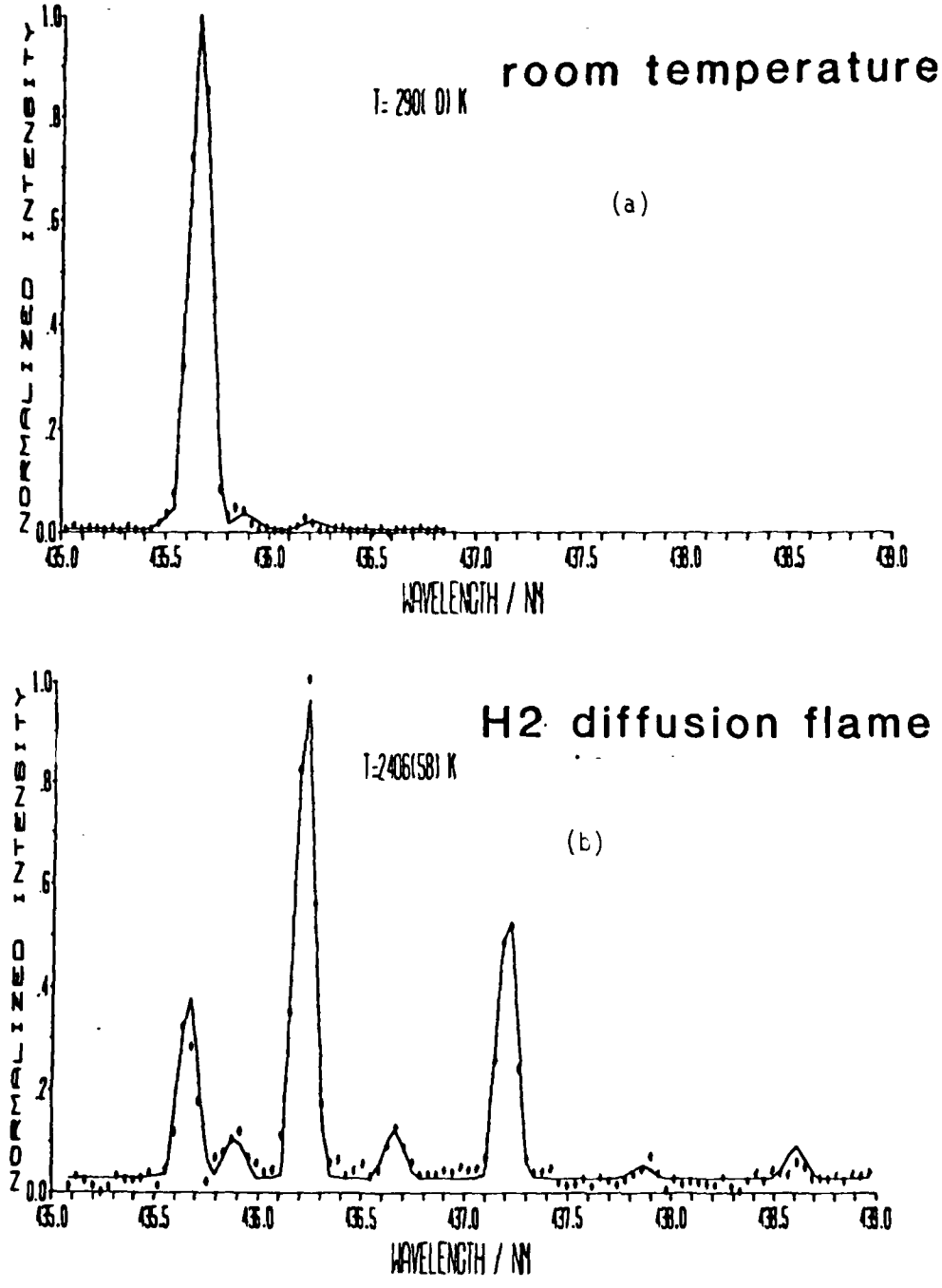

Figure 12. H_2 CARS spectra obtained in various environments using a 2360 groove/mm grating giving a resolution of about 5 cm^{-1}; (a) pure H_2 at room temperature using BOXCARS geometry, (b) a H_2 diffusion flame using BOXCARS geometry.

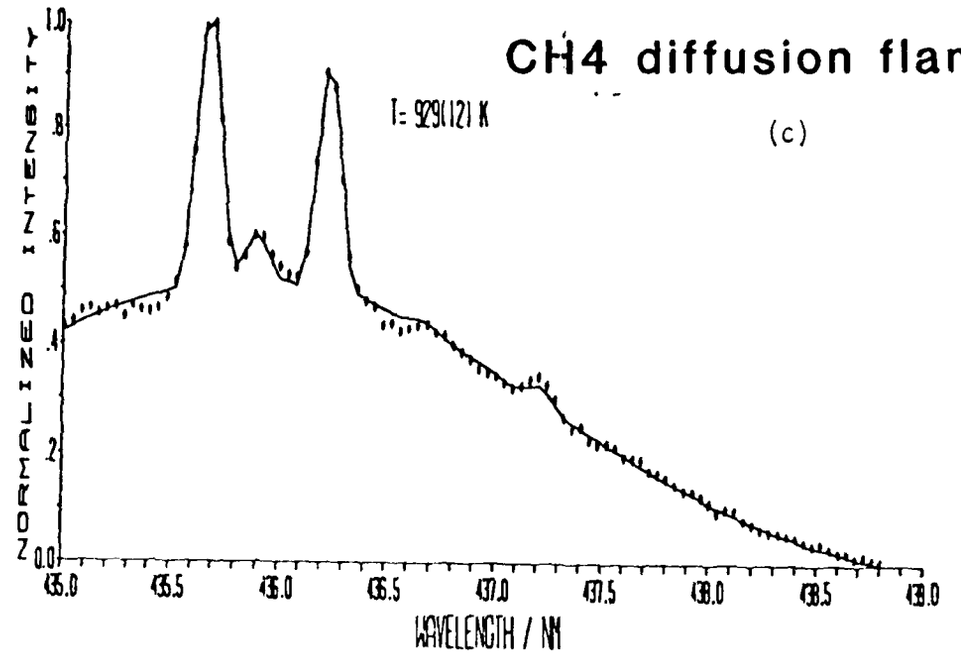

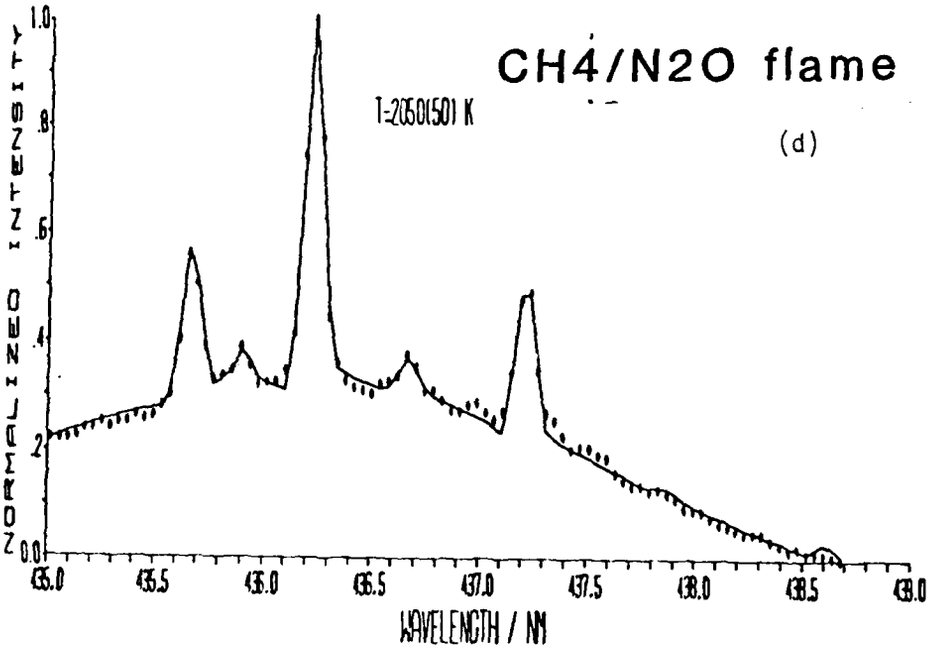

Figure 12 continued; (c) a CH_4 diffusion flame using collinear geometry and (d) a rich CH_4/N_2O flame using collinear geometry.

Figs. 12c and 12d show H_2 CARS signals obtained in a relatively cool part of a CH_4 diffusion flame and a rich CH_4/N_2O flame, respectively. In these cases much smaller quantities of H_2 were present for CARS signal generation and collinear geometry was employed to obtain sufficient signal. The measurements were made 6 mm above the porous plug burner surface using 33 laser shots and an unattenuated CARS signal beam. The broad underlying background is the manifestation of the CARS signal generated by the non-resonant susceptibility. A useful feature of this broad curve is that it tracks the dye laser output which is now conveniently observed at the anti-Stokes frequency and thus can be used to gauge exactly where the dye laser is peaked as well as its overall shape for that experimental run. It can be seen that the H_2 spectra in Figs. 12c and 12d are not perturbed to any extent by the non-resonant susceptibility other than sitting on a broad background. This observation can be explained as follows. In collinear geometry the laser beams are also overlapped in the room air surrounding the flame and this results in generation of CARS signals. However, the frequencies of the lasers have been set for resonance conditions for H_2, thus only non-resonance CARS signals appear from the room air (N_2 and O_2). This is the dominant contribution to the non-resonant signal, a place where there is no H_2, thus no mixing of resonant H_2 CARS signals occur. If the dominant non-resonant contribution were occurring inside the flame where H_2 is also present, then an obvious perturbation of the H_2 spectrum would result. The computer fits for Figs. 12c and 12d include only a non-resonant susceptibility contribution outside the flame. An attempt to fit the experimental data of Fig. 12d with the non-resonant contribution occuring only inside the flame is shown in Fig. 13. Clearly this results in a poor fit and an unreasonably high temperature. The double asterisk for the standard deviation indicates that more than two digits are required.

VI. CONCLUSIONS AND RECOMMENDATIONS

CARS spectroscopy has been used to determine the temperature and temperature profiles in several laboratory flames. CARS signals from both N_2 and H_2 have been used in these determinations. This technique is capable of high temporal (10^{-8}s) and spatial ($1mm^3$) resolution. Although the CARS technique is straightforward, it is much more complex both experimentally and computationally than spontaneous Raman spectroscopy[39], another technique also used in this laboratory. For relatively clean steady state flames sufficient signals are generated from the spontaneous Raman effect to determine both temperature and major species concentrations and thus is the preferred choice of techniques. The CARS technique usually exhibits greater advantages when applied to the more hostile environments. Probably the biggest single advantage of CARS is that the signal emerges as a laser-like beam rather than dispersed over 4 π steradians. Thus one can collect all the signal remotely, without capturing a large amount of unwanted noise signals. In the field of ballistics several types of environments may be suited for probing with the CARS technique. These environments are hot gases exhausting from guns (muzzle flash problem) and propellants burning within a strand burner. The next several paragraphs expand on these possible applications.

---

[39] *J.A. Vanderhoff, R.A. Beyer and A.J. Kotlar, "Laser Raman Spectroscopy of Flames: Temperature and Concentrations in CH_4/N_2O Flames," Technical Report ARBRL-TR-02388, January 1982.*

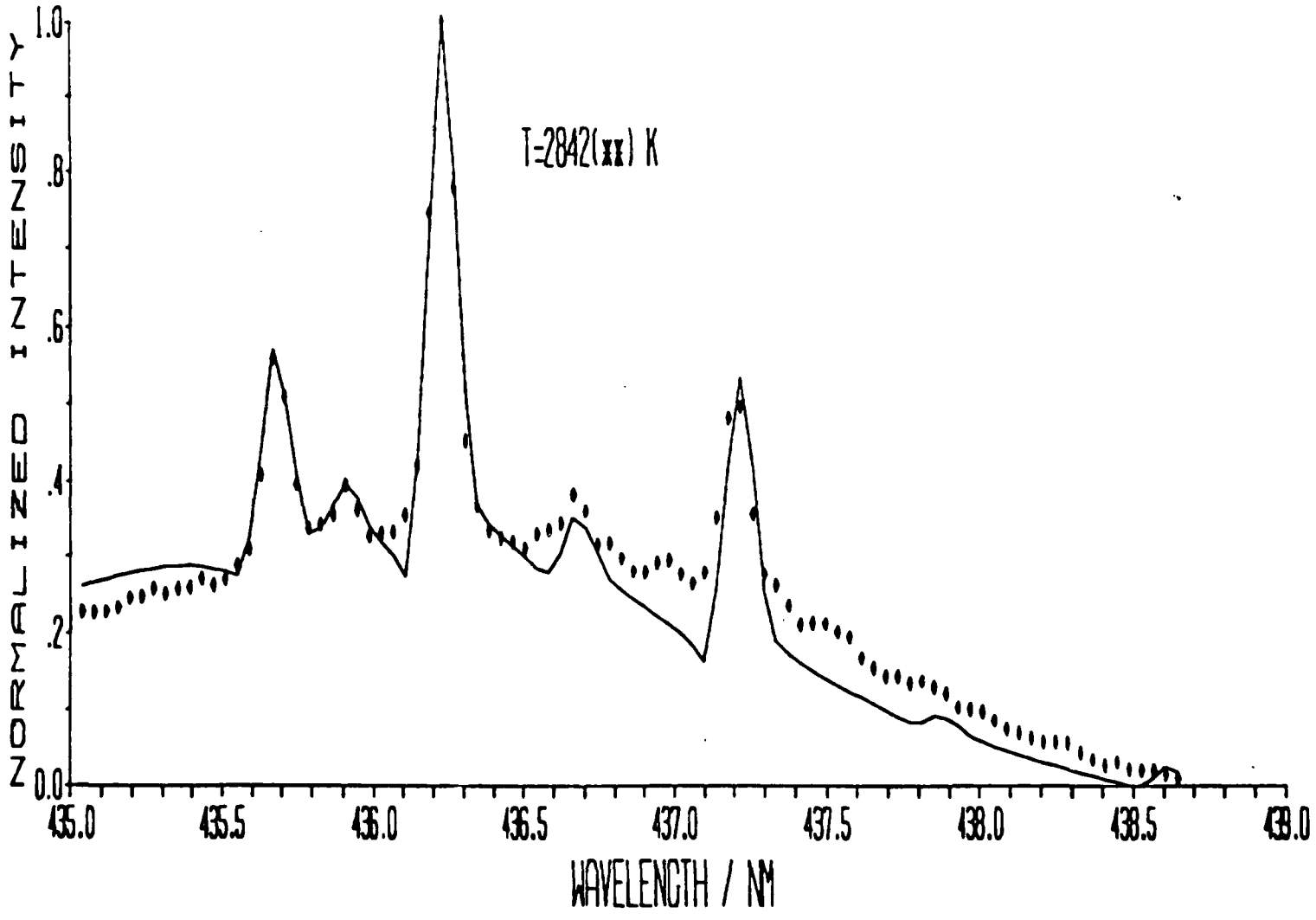

Figure 13. A repeat of the experimental data of Fig. 12d, however in this case an attempt was made to computer fit the spectrum with a non-resonant susceptibility contribution from only within the flame.

Secondary muzzle flash results from the burning of fuel rich exhaust gases with entrained ambient air. Klingenberg[40] has made measurements of temperature, gas velocity, and pressure in secondary flash produced from a 7.62 mm rifle. The time frame he observes is from 1 to 3.4 ms after the exit of the projectile. Here pressures are close to 1 atmosphere and for firing into ambient air the temperatures are in the 2000K range with quoted errors of ± 8% for these sodium and potassium line-reversal methods of temperature determination. The major exhaust gas species are H_2O, CO, CO_2, H_2 and N_2. The concentration of these species come, almost universally, from the results of thermochemical equilibrium calculations rather than experimental measurements. All of these gases have been previously investigated in a laboratory environment using the CARS technique. Since the pressure, temperature, and composition of gases in the vicinity of muzzle flash are similar to those of the laboratory flames discussed in the text, the CARS signal should be about as large thus amenable for single shot data with a temporal resolution of 10^{-8}s. Additionally, collinear geometry CARS can be used with ease for all of the molecules except N_2 thus simplifying optical alignment while producing substantially more CARS signal then for BOXCARS geometry. With CARS, single shot temperature measurements to an accuracy of ±2% should be realizable. Concentrations of the major species can also be obtained from the spectral shape of the CARS signal (see for example Ref. 17). Obtaining concentrations from CARS signals has not been investigated as much as temperature determinations; thus probable error limits are not reported here. One disadvantage of this technique should be pointed out. Although excellent temporal and spatial resolution can be obtained, it would be possible to use only one laser shot per firing. High power Nd:YAG lasers operate at repetition rates on the order of 10 Hz and the time scale of interest for secondary muzzle flash is milliseconds. A high power laser operating at 1 kHz would be very desirable, however, commercial laser technology has not yet advanced to this point.

The other potential application of CARS is to study properties of propellant burning experimentally. Harris and McIlwain[16] have measured the temperature above an unconfined propellant burning in room air using the CARS signal from N_2. This environment is totally different from the gun barrel environment of interest. An environment which better simulates propellant burning but not as hostile as the gun barrel is a strand burner. The strand burner was designed to measure the burning rate of propellants as a function of pressure. It is a vessel where the pressure,initial temperature, and gas composition are controllable[41]. Two optical ports on this vessel would allow a CARS experiment to be conducted. Temperature and major species concentrations (H_2, CO, N_2, H_2O, CO_2, N_2O, NO_2, NO and HCN) could be obtained as a function of various parameters such as pressure, distance from the propellant surface, etc. It must be noted however, that due to probable

---

[40] *G. Klingenburg, "Investigation of Combustion Phenomena Associated with the Flow of Hot Propellant Gases. III: Experimental Survey of the Formation and Decay of Muzzle Flow Fields and of Pressure Measurements," Combustion and Flame, Vol. 29, pp. 289-309, 1977.*

[41] *N. Kubota, T.J. Ohlemiller, L.H. Caveny and M. Summerfield, "The Mechanism of Super-Rate Burning of Catalyzed Double Base Propellants," Aerospace and Mechanical Sciences Report Number 1087, 1973, Princeton University, New Jersey.*

uneven burning of the propellant surface, distances less than a millimeter from the surface cannot be reliably probed with a double-ended optical technique such as CARS; thus it is not likely that surface temperatures or initial formation of species can be obtained at pressures greater than about one atmosphere when the reaction zone extent is in the submillimeter region. Nonetheless, farther from the propellant surface, temperatures and concentration measurements are feasible and can be compared against current thermochemical equilibrium codes to assess their validity. Multiple data points can be obtained from each strand burning since at atmospheric pressure the propellant burning rate is on the order of 0.1 cm/sec and the region of interest is about 1 cm. Some information may also be obtained at elevated pressure where the CARS signal can increase dramatically. This increase is proportional to various powers of density (N) depending on which molecular linewidth regime applies; N for pressure broadening, N^2 for Doppler broadening, and N^3 for motional narrowing. For further details on the effects see Refs. 38 and 42.

Current efforts[43] are underway to model the high pressure CARS signals for various molecules well enough to extract accurate temperatures and concentrations.

---

[42] *R.J. Hall, J.F. Verdieck and A.C. Eckbreth, "Pressure-Induced Narrowing of the CARS Spectrum of N_2," Opt. Comm., Vol. 35, p. 69, 1980.*

[43] *A. Eckbreth, "CARS Diagnostics of High Pressure Combustion," ARO Contract DAA29-79-C-0008, Feb. 1979 - Feb. 1982.*

REFERENCES

1. M. Lapp and C.M. Penney, Eds., Laser Raman Gas Diagnostics, Plenum Press, New York, 1973.

2. S. Lederman, "The Use of Laser Raman Diagnostics in Flow Fields and Combustion," Prog. Energy Combust. Sci., Vol. 3, pp. 1-34, 1977.

3. M. Lapp, "Raman Scattering Measurements of Combustion Properties," Laser Probes for Combustion Chemistry, ACS Symposium Series 134, Washington, D.C., 1980.

4. J.H. Bechtel, "Temperature Measurements of the Hydroxyl Radical and Molecular Nitrogen in Premixed Laminar Flames by Laser Techniques," Applied Optics, Vol. 18, p. 2100, 1979.

5. M. Bridoux, M. Crunell-Cras, F. Grase, and Michel Delhaye, "Use of Multichannel Pulsed Raman Spectroscopy as a Diagnostic Technique in Flames," Combustion and Flame, Vol. 36, pp. 109-116, 1979.

6. M.C. Drake and G.M. Rosenblatt, "Rotational Raman Scattering from Premixed and Diffusion Flames," Combustion and Flame, Vol. 33, pp. 179-196, 1978.

7. G. Alessandretti, "Some Results on the Measurement of Temperature and Density in a Flame by Raman Spectroscopy," Optica Acta, Vol. 27, pp. 1095-1103, 1980.

8. A.A. Boiarski, R.H. Barnes, and J.F. Kircher, "Flame Measurements Utilizing Raman Scattering," Combustion and Flame, Vol. 32, pp. 111-114, 1978.

9. D.P. Aeschliman, J.C. Cummings, and R.A. Hill, "Raman Spectroscopic Study of a Laminar Hydrogen Diffusion Flame in Air," J. Quant. Spectrosc. Radiat. Transfer, Vol. 21, pp. 293-307, 1979.

10. A.C. Eckbreth, P.A. Bonczyk, and J.F. Verdieck, "Laser Raman and Fluorescence Techniques for Practical Combustion Diagnostics," Appl. Spectros. Reviews, Vol. 13, p. 15-164, 1978.

11. J.W. Nibler and G.V. Knighten, "Coherent Anti-Stokes Raman Spectroscopy," Raman Spectroscopy of Gases and Liquids, Topics in Current Physics, Vol. II, Springer-Verlag, New York, 1979.

12. A.C. Eckbreth, R.J. Hall, and J.A. Shirley, "Investigations of Coherent Anti-Stokes Raman Spectroscopy (CARS) for Combustion Diagnostics," AIAA Paper 79-0083 17th Aerospace Sciences Meeting, New Orleans, LA., Jan. 1979.

13. A.C. Eckbreth, "CARS Thermometry in Practical Combustors," Combustion and Flame, Vol. 39, pp. 133-147, 1980.

REFERENCES

14. G.L. Switzer, L.P. Goss, W.M. Roquemore, R.P. Bradley, P.W. Schreiber,and W.B. Roh, "Application of CARS to Simulated Practical Combustion Systems," Journal of Energy,Vol. 4, p. 209, 1980.

15. I.A. Stenhouse, D.R. Williams, J.B. Cade, and M.P. Swords, "CARS in an Internal Combustion Engine," Applied Optics, Vol. 18, pp. 3819 1979.

16. L.E. Harris and M.E. McIlwain, "CARS Spectroscopy of Gun Propellant Flames," Technical Report ARLCD-TR-81007, 1981.

17. A.C. Eckbreth and R.J. Hall, "CARS Concentration Sensitivity With and Without Nonresonant Background Suppression," Combustion Science and Technology, Vol. 25, pp. 175-192, 1981.

18. M. Pealat, B. Attal, and J.P.E. Taran, "CARS Diagnostics of Combustion," AIAA 80-0282, 1980.

19. L.A. Rahn, L.J. Zych, and P.L. Mattern, "Background-free CARS Studies of Carbon Monoxide in a Flame," Optical Communications Vol. 39, p. 249, 1979.

20. P.D. Maker and R.W. Terhune, "Study of Optical Effects Due to an Induced Polarization Third Order in the Electric Field Strength," Phys. Rev.Vol. 137, pp. A801-A818, 1965.

21. P.R. Regnier and J.P.E. Taran, "On the Possibility of Measuring Gas Concentrations by Stimulated Anti-Stokes Scattering," Appl. Phys. Lett., Vol. 23, pp. 240-242, 1973.

22. S.A. Akhmanov and N.I. Koroteev, "Spectroscopy of Light Scattering and Nonlinear Optics. Nonlinear-Optical Methods of Active Spectroscopy of Raman and Rayleigh Scattering," Sov. Phys. Usp. Vol. 20, pp. 899-936, 1977.

23. W.M. Tolles, J.W. Nibler, J.R. MacDonald, and A.B. Harvey, "A Review of the Theory and Application of Coherent Anti-Stokes Raman Spectroscopy (CARS)," Applied Spectroscopy Vol. 31, pp. 253-271 1977.

24. A.C. Eckbreth, "BOXCARS: Crossed-Beam Phase-Matched CARS Generation in Gases," Appl. Phys. Lett. Vol. 32, pp. 421-423, 1978.

25. J.A. Shirley, R.J. Hall, and A.C. Eckbreth, "Folded BOXCARS for Rotational Raman Studies," Optics Letters, Vol. 5, pp. 380-382 1980.

26. M.D Levenson and N. Bloembergen, "Dispersion of the Nonlinear Optical Susceptibility Tensor in Centrosymmetric Media," Phys. Rev. B Vol. 10, pp.4447-4463, 1974.

27. R.L. Farrow, R.E. Mitchell, L.A. Rahn, and P.L. Mattern, "Crossed-Beam Background-Free CARS Measurements in a Methane Diffusion Flame," AIAA-81-0182, 1981.

28. Polarization of ω_1 can be made either horizontal or vertical by orientation of the frequency doubling crystal. To obtain essentially one polarization in the dye laser a Glan-air prism can be inserted in the oscillator cavity and thus the polarization can be changed by orientation of this prism.

29. A.J. Kotlar, R.W. Field, J.I. Steinfeld and J.A. Coxon, "Analysis of Perturbations in the $A^2\pi - X^2\Sigma^+$ Red System of CN," Journal of Molecular Spectroscopy, Vol. 80, pp.86-108, 1980.

30. A.J. Kotlar and J.A. Vanderhoff, "A Model for the Interpretation of CARS Experimental Profiles," accepted for publication in Applied Spectroscopy, "Interpretation and Least Squares Fitting of CARS Experimental Profiles." BRL Report in preparation.

31. K.P. Huber and G. Herzberg, "Molecular Spectra and Molecular Structure IV. Constants of Diatomic Molecules," Van Nostrand Reinhold Company, New York, 1979.

32. U. Fink, T.A. Wiggins and D.H. Rank, "Frequency and Intensity Measurements on the Quadrupole Spectrum of Molecular Hydrogen," J. Mol. Spectrosc., Vol. 18, p. 384, 1965.

33. J.V. Flotz, D.H. Rank and T.A. Wiggins, "*Determinations of Some* Hydrogen Molecular Constants," J. Mol. Spectrosc., Vol. 21, p. 203 1966.

34. R.A. Svehla and B.J. McBride, "Fortran IV Computer Program for Calculation of Thermodynamic and Transport Properties of Complex Chemical Systems," NASA TN D-7056, 1973.

35. This effect has been observed in our laboratory whenever using porous plug burners in spontaneous Raman and fluorescence studies. See for example W.R. Anderson, L.J. Decker, and A.J. Kotlar, "Temperature Profile of a Stoichiometric CH_4/N_2O Flame from Laser Excited Fluorescence Measurements on OH," accepted for publication in Combustion and Flame.

36. G. Herzberg, Spectra of Diatomic Molecules, (Van Nostrand Reinhold, New York, 1950).

37. It was stated earlier that the burner head cooled the flame substantially. This holds true only for premixed flames where the flame is stabilized on the burner head. In the diffusion flames where room air is the oxidant, the reaction zone is cone shaped due to the way the air mixes with the fuel. Around the tip of the cone (40 mm) where the measurement was made there is negligible heat loss to the burner.

REFERENCES

38. J.A. Shirley, A.C. Eckbreth, and R.J. Hall, "Investigation of the Feasibility of CARS Measurements in Scramjet Combustion," UTRC Report R79-954390-8, 1979.

39. J.A. Vanderhoff, R.A. Beyer and A.J. Kotlar, "Laser Raman Spectroscopy of Flames: Temperature and Concentrations in CH_4/N_2O Flames," Technical Report ARBRL-TR-02388, January 1982.

40. G. Klingenburg, "Investigation of Combustion Phenomena Associated with the Flow of Hot Propellant Gases. III: Experimental Survey of the Formation and Decay of Muzzle Flow Fields and of Pressure Measurements," Combustion and Flame Vol. 29, pp. 289-309, 1977.

41. N. Kubota, T.J. Ohlemiller, L.H. Caveny and M. Summerfield, "The Mechanism of Super-Rate Burning of Catalyzed Double Base Propellants," Aerospace and Mechanical Sciences Report Number 1087, 1973, Princeton University, New Jersey.

42. R.J. Hall, J.F. Verdieck and A.C. Eckbreth, "Pressure-Induced Narrowing of the CARS Spectrum of N_2," Opt. Comm. Vol. 35, p. 69 1980.

43. A. Eckbreth, "CARS Diagnostics of High Pressure Combustion," ARO Contract DAA29-79-C-0008, Feb. 1979 - Feb. 1982.

DISTRIBUTION LIST

No. of Copies	Organization
12	Administrator Defense Technical Info Center ATTN: DTIC-DDA Cameron Station Alexandria, VA 22314
1	Director Defense Advanced Research Projects Agency ATTN: LTC C. Buck 1400 Wilson Boulevard Arlington, VA 22209
2	Director Inst for Defense Analysis ATTN: H. Wolfhard R.T. Oliver 1801 Beauregard St. Alexandria, VA 22311
1	Commander US Army Materiel Development and Readiness Command ATTN: DRCDMD-ST 5001 Eisenhower Avenue Alexandria, VA 22333
2	Commander US Army Armament Research and Development Command ATTN: DRDAR-TSS Dover, NJ 07801
5	Commander US Army Armament Research and Development Command ATTN: DRDAR-LCA, D.Downs DRDAR-LC, L. Harris DRDAR-SCA, L.Stiefel DRDAR-LCE, R.F. Walker DRDAR-TDC, D.Gyorog Dover, NJ 07801
1	Commander US Army Armament Materiel Readiness Command ATTN: DRSAR-LEP-L, Tech Lib Rock Island, IL 61299
1	Director US Army ARRADCOM Benet Weapons Lab ATTN: DRDAR-LCB-TL Watervliet, NY 12189
1	Commander US Army Watervliet Arsenal ATTN: Code SARWV-RD, R. Thierry Watervliet, NY 12189
1	Commander US Army Aviation Research and Development Command ATTN: DRDAV-E 4300 Goodfellow Blvd St. Louis, MO 63120
1	Director US Army Air Mobility Research and Development Laboratory Ames Research Center Moffett Field, CA 94035
1	Commander US Army Communications Rsch and Development Command ATTN: DRDCO-PPA-SA Fort Monmouth, NJ 07703
1	Commander US Army Electronics Research and Development Command Technical Support Activity ATTN: DELSD-L Fort Monmouth, NJ 07703
1	Commander US Army Missile Command ATTN: DRSMI-R Redstone Arsenal, AL 35898
1	Commander US Army Missile Command ATTN: DRSMI-YDL Redstone Arsenal, AL 35898

DISTRIBUTION LIST

No. of Copies	Organization
1	Commander US Army Natick Research and Development Command ATTN: DRXRE, D.Sieling Natick, MA 01762
1	Commander US Army Tank Automotive Research & Development Cmd ATTN: DRDTA-UL Warren, MI 48090
1	Commander US Army White Sands Missile Range ATTN: STEWS-VT White Sands, NM 88002
1	Commander US Army Materials and Mechanics Research Center ATTN: DRXMR-ATL Watertown, MA 02172
5	Commander US Army Research Office ATTN: Tech Lib D. Squire F. Schmiedeshaff R. Ghirardelli M. Ciftan P.O. Box 12211 Research Triangle Park NC 27706
1	Director US Army TRADOC Systems Analysis Activity ATTN: ATAA-SL, Tech Lib White Sands Missile Range, NM 88002
2	Office of Naval Research ATTN: Code 473 G. Neece 800 N. Quincy Street Arlington, VA 22217
1	Commander Naval Sea Systems Command ATTN: J.W. Murrin,SEA-62R2 National Center Bldg 2, Room 6E08 Washington, D.C. 20362
1	Commander Naval Surface Weapons Center ATTN: Library Br., DX-21 Dahlgren, VA 22448
2	Commander Naval Surface Weapons Center ATTN: S.J.Jacobs/Code 240 Code 730 Silver Spring, MD 20910
1	Commander Naval Underwater Systems Cmd Energy Conversion Department ATTN: R.S.Lazar/Code 5B331 Newport, RI 02840
2	Commander Naval Weapons Center ATTN: R. Derr C. Thelen China Lake, CA 93555
1	Commander Naval Research Laboratory ATTN: Code 6180 Washington, DC 20375
1	Commander Naval Research Laboratory Chem. Division ATTN: J. McDonald Washington, DC 20375
1	Sandia National Laboratories ATTN: D. Stephenson Div 8351 Livermore, CA 94550

DISTRIBUTION LIST

No. of Copies	Organization
3	Superintendent Naval Postgraduate School ATTN: Tech Lib D. Netzer A. Fuhs Monterey, CA 93940
2	Commander Naval Ordnance Station ATTN: Dr. Charles Dale Tech Lib Indian Head, MD 20640
2	AFOSR ATTN: D. Ball L. Caveny Bolling AFB, DC 20332
2	AFRPL(DYSC) ATTN: D. George J.N. Levine Edwards AFB, CA 93523
5	National Bureau of Standards ATTN: J. Hastie T. Kashiwagi H. Semerjian M. Jacox J. Stevenson Washington, DC 20234
1	General Motors Rsch Labs Physics Department ATTN: J.H. Bechtel Warren, Michigan 48090
1	Lockheed Missiles & Space Co ATTN: Tech Info Ctr 3521 Hanover Street Palo Alto, CA 94304
1	System Research Labs ATTN: L. Goss 2600 Indian Ripple Rd Dayton, Ohio 45440
1	Aerojet Solid Propulsion Co ATTN: P. Micheli Sacramento, CA 95813
1	ARO Incorporated ATTN: N. Dougherty Arnold AFS, TN 37389
1	Atlantic Research Corporation ATTN: M.K. King 5390 Cherokee Avenue Alexandria, VA 22314
1	AVCO Everett Research Lab Div ATTN: D. Stickler 2385 Revere Beach Parkway Everett, MA 02149
2	Calspan Corporation ATTN: E.B. Fisher A.P. Trippe P.O. Box 400 Buffalo, NY 14225
2	Exxon Research & Engineering ATTN: A. Dean M. Chou P.O. Box 45 Linden, NJ 07036
1	Foster Miller Associates ATTN: A.J. Erickson 135 Second Avenue Waltham, MA 02154
1	General Electric Company Armament Department ATTN: M.J. Bulman Lakeside Avenue Burlington, VT 05402
1	General Electric Company Flight Propulsion Division ATTN: Tech Lib Cincinnati, OH 45215

DISTRIBUTION LIST

No. of Copies	Organization
1	General Electric Corp R&D ATTN: M. Drake P.O. Box 8, Bldg K1 Room 51326 Schenectady, NY 12301
2	Hercules Powder Co Allegheny Ballistics Lab ATTN: R. Miller Tech Lib Cumberland, MD 21501
1	Hercules Incorporated Bacchus Works ATTN: B. Isom Magna, UT 84044
1	IBM Corp ATTN: A.C. Tam Research Division 5600 Cottle Rd San Jose, CA 95193
1	IITRI ATTN: M.J. Klein 10 West 35th Street Chicago, IL 60616
1	Olin Corporation Badger Army Ammunition Plant ATTN: J. Ramnarace Baraboo, WI 53913
1	Physics International 2700 Merced Street Leandro, CA 94577
1	Paul Gough Associates, Inc ATTN: P.S. Gough P.O. Box 1614 Portsmouth, NH 03801
1	United Technologies ATTN: A.C. Eckbreth East Hartford, CT 06108
1	Pulsepower Systems, Inc ATTN: L.C. Elmore 815 American Street San Carlos, CA 94070
3	Rockwell International Corp Rocketdyne Division ATTN: C. Obert J.E. Flanagan A. Axeworthy 6633 Canoga Avenue Canoga Park, CA 91304
2	Hercules, Inc Industrial Systems Dept ATTN: W. Haymes Tech Lib McGregor, TX 76657
1	Science Applications, Inc ATTN: R.B. Edelman Combustion Dynamics & Propulsion Division 23146 Cumorah Crest Woodland Hills, CA 91364
1	Shock Hydrodynamics, Inc ATTN: W.H. Anderson 4710-16 Vineland Avenue N. Hollywood, CA 91602
1	Thiokol Corporation Elkton Division ATTN: E. Sutton Elkton, MD 21921
3	Thiokol Corporation Huntsville Division ATTN: D. Flanigan R. Glick Tech Lib Huntsville, AL 35807
2	Thiokol Corporation Wasatch Division ATTN: J. Peterson Tech Lib P.O. Box 524 Brigham City, UT 84302

DISTRIBUTION LIST

No. of Copies	Organization
1	TRW Systems Group ATTN: H. Korman One Space Park Redondo Beach, CA 90278
2	United Technologies Chemical Systems Division ATTN: R. Brown Tech Lib P.O. Box 358 Sunnyvale, CA 94086
3	Battelle Memorial Institute ATTN: Tech Lib 505 King Avenue Columbus, OH 43201
2	Brigham Young University Dept of Chemical Engineering ATTN: M.W. Beckstead Provo, UT 84601
1	California Institute of Tech 204 Karmar Lab Mail Stop 301-46 ATTN: F.E.C. Culick 1201 E. California Street Pasadena, CA 91125
1	Case Western Reserve Univ Aerospace Sciences ATTN: J. Tien Cleveland, OH 44135
1	Cornell University Dept of Chemistry ATTN: E. Grant Ithaca, NY 14853
3	Georgia Institute of Tech School of Aerospace Eng ATTN: B.T. Zinn E. Price W.C. Strahle Atlanta, GA 30332
1	Institute of Gas Technology ATTN: D. Gidaspow 3424 S. State Street Chicago, IL 60616
1	John Hopkins University/APL Chemical Propulsion Info Ag ATTN: T. Christian John Hopkins Road Laurel, MD 20707
1	Massachusetts Inst of Tech Dept of Mech Engineering ATTN: T. Toong Cambridge, MA 02139
2	Pennsylvania State University Dept of Mechanical Eng ATTN: K. Kuo G. Faeth University Park, PA 16802
1	Pennsylvania State University Department of Material Sciences ATTN: H. Palmer University Park, PA 16802
1	Polytechnic Institute of NY ATTN: S. Lederman Route 110 Farmingdale, NY 11735
1	Princeton Combustion Research Laboratories ATTN: M. Summerfield 1041 US Highway One North Princeton, NJ 08540
3	Princeton University Forrestal Campus ATTN: I. Glassman K. Brezinsky Tech Lib P.O. Box 710 Princeton, NJ 08540

DISTRIBUTION LIST

No. of Copies	Organization
4	Purdue University School of Mechanical Eng ATTN: J. Osborn S.N.B. Murphy N.M. Laurendeau D.Sweeney TSPC Chaffee Hall W. Lafayette, IN 47906
1	Rensselaer Polytechnic Inst Dept of Chem Engineering ATTN: A. Fonijn Troy, NY 12181
1	Rutgers State University Dept of Mechanical and Aerospace Engineering ATTN: S. Temkin University Heights Campus New Brunswick, NJ 08903
1	Sandia Laboratories Combustion Sciences Dept ATTN: R. Cattolica Livermore, CA 94550
4	SRI International ATTN: Tech Lib D. Crosley J. Barker D. Golden 33 Ravenswood Avenue Menlo Park, CA 94025
1	Stevens Institute of Tech Davidson Library ATTN: R. McAlevy, III Hoboken, NJ 07030
1	University of California, San Diego Ames Department ATTN: F. Williams P.O. Box 109 La Jolla, CA 92037
1	University of California Dept of Mechanical Eng ATTN: J.W.Daily Berkeley, California 94720
1	Univ of Dayton Rsch Inst ATTN: D. Campbell AFRPL/PAP Stop 24 Edwards AFB, CA 93523
1	University of Florida Dept of Chemistry ATTN: J. Winefordner Gainesville, Florida 32611
1	University of Illinois Dept of Mechanical Eng ATTN: H. Krier 144 MEB, 1206 W. Green St Urbana, IL 61801
1	University of Minnesota Dept of Mechanical Eng ATTN: E. Fletcher Minneapolis, MN 55455
1	University of Southern California Department of Chemistry ATTN: S. Benson Los Angeles, CA 90007
2	University of Texas Department of Chemistry ATTN: W. Gardiner H. Schaefer Austin, TX 78712
2	University of Utah Dept of Chemical Engineering ATTN: A. Baer C. Flandro Salt Lake City, UT 84112

DISTRIBUTION LIST

No. of Copies	Organization
1	Stanford University Dept of Chemistry ATTN: John Ross Stanford, CA 94305
1	Colorado State University Dept of Physics ATTN: Chia-Yao She Fort Collins, Colorado 80523

ABERDEEN PROVING GROUND

Dir, USAMSAA
ATTN: DRXSY-D
DRXSY-MP, H. Cohen

Cdr, USATECOM
ATTN: DRSTE-TO-F

Dir, USACSL, Bldg E3516
ATTN: DRDAR-CLB-PA